

Prenatal treprostinil improves pulmonary arteriolar hypermuscularization in the rabbit model of congenital diaphragmatic hernia

Felix R. De Bie^a, Yannick Regin^b, Antoine Dubois^c, Marianna Scuglia^a, Tomohiro Arai^a, Ewout Muylle^a, David Basurto^a, Marius Regin^d, Siska Croubels^e, Marc Cherlet^e, Emily A. Partridge^f, Karel Allegaert^{b,g,h}, Francesca M. Russo^{a,i}, Jan A. Deprest^{a,i,j,*}

^a Unit of Urogenital, Abdominal and Plastic Surgery, Department of Development and Regeneration, KU Leuven, Belgium

^b Unit of Woman and Child, Department of Development and Regeneration, KU Leuven, Belgium

^c Unit of Abdominal Transplantation, Department of Microbiology, Immunology and Transplantation, KU Leuven, Belgium

^d Research Group Reproduction and Genetics, Vrije Universiteit Brussel, Belgium

^e Department of Pathobiology, Pharmacology and Zoological Medicine, Laboratory of Pharmacology and Toxicology, Faculty of Veterinary Medicine, Ghent University, Merelbeke, Belgium

^f Center for Fetal Research, The Children's Hospital of Philadelphia, United States

^g Department of Pharmaceutical and Pharmacological Sciences, KU Leuven, Leuven, Belgium

^h Department of Hospital Pharmacy, Erasmus MC, Rotterdam, the Netherlands

ⁱ Division of Obstetrics and Gynecology, University Hospitals Leuven, Belgium

^j Institute for Women's Health, University College London, United Kingdom

ARTICLE INFO

Keywords:

Foetal therapy – pulmonary hypertension – congenital diaphragmatic hernia - treprostinil

ABSTRACT

Congenital diaphragmatic hernia (CDH) is a congenital malformation characterized by pulmonary hypoplasia, pulmonary hypertension, and cardiac dysfunction. Pulmonary hypertension represents the major cause of neonatal mortality and morbidity. Prenatal diagnosis allows assessment of severity and selection of foetal surgery candidates. We have shown that treprostinil, a prostacyclin analogue with an anti-remodelling effect, attenuates the relative hypermuscularization of the pulmonary vasculature in rats with nitrofen-induced CDH. Here we confirm these observations in a large animal model of surgically-created CDH. In the rabbit model, subcutaneous maternal administration of treprostinil at 150 ng/kg/min consistently reached target foetal concentrations without demonstrable detrimental foetal or maternal adverse effects. In pups with CDH, prenatal treprostinil reduced pulmonary arteriolar proportional medial wall thickness and downregulated inflammation and myogenesis pathways. No effect on alveolar morphometry or lung mechanics was observed. These findings provide further support towards clinical translation of prenatal treprostinil for CDH.

Research in context

Evidence before this study

Persistent pulmonary hypertension causes significant mortality and morbidity in infants with congenital diaphragmatic hernia (CDH). Foetal endoluminal tracheal occlusion is currently the only validated foetal therapy for CDH, however is associated with higher rates of pre-term delivery and its effect on pulmonary vascular development has not been fully elucidated. We therefore investigated a prenatal, pharmacologic, non-invasive therapy specifically targeting pulmonary vascular development in CDH. Treprostinil has demonstrated antiremodeling effects on pulmonary vascular smooth muscles cells demonstrated in vitro, and in a nitrofen rat model of CDH prenatal treprostinil has

been demonstrated to reduce the pulmonary hypertensive phenotype.

Added value of this study

We herein demonstrate that (1) treprostinil's antiremodeling receptors are expressed at relevant foetal age, (2) treprostinil administration during the pseudo-glandular lung development phase is well tolerated by the mother and the foetus, and (3) prenatal maternal treprostinil administration reduces the pulmonary arteriolar hypermuscularization in foetal rabbit pups with surgically-induced CDH, downregulates inflammation and myogenesis pathways, improving the pulmonary hypertensive phenotype. This study corroborates previous findings in the nitrofen rat model, now in a higher species, which is closer to humans in terms of pulmonary development, providing

* Corresponding author.

E-mail address: jan.deprest@uzleuven.be (J.A. Deprest).

<https://doi.org/10.1016/j.bioph.2023.115996>

Received 12 September 2023; Received in revised form 28 November 2023; Accepted 6 December 2023

Available online 12 December 2023

0753-3322/© 2023 The Authors. Published by Elsevier Masson SAS. This is an open access article under the CC BY-NC-ND license (<http://creativecommons.org/licenses/by-nc-nd/4.0/>).

essential information on the safety and efficacy of treprostinil, and clearing the way towards clinical translation.

Implications of all the available evidence

This study provides evidence of safety and efficacy of prenatal treprostinil treatment in CDH in a second, higher animal model of CDH, paving the way for clinical investigation of the potential of prenatal treprostinil administration to improve prenatal pulmonary vascular development in CDH.

1. Introduction

Congenital diaphragmatic hernia (CDH) is a rare congenital malformation (2.3/10,000 live births) characterized by a diaphragmatic defect allowing herniation of abdominal viscera into the chest, resulting in compression of the developing lungs and heart[1]. The pathophysiology of CDH is characterized by airway hypoplasia, pulmonary vascular remodelling, and cardiac dysfunction. After birth this results in impaired gas exchange, pulmonary hypertension (PH) and ventricular dysfunction[2–4]. Despite improvements in neonatal intensive care, refractory PH accounts for most CDH-related mortality and morbidity[4]. CDH can be diagnosed prior to birth, and the severity of pulmonary hypoplasia assessed. Adverse structural pulmonary changes in CDH have been shown to develop in utero, making foetal treatment of pulmonary hypoplasia a promising therapeutic strategy. Clinically, Foetoscopic Endoluminal Tracheal Occlusion (FETO) has been demonstrated to improve survival in selected fetuses[5,6]. However, experimental studies have demonstrated that FETO mainly addresses airway hypoplasia[7–9]. Prenatal therapy to reverse abnormal vascular development would represent a breakthrough in CDH treatment. Ideally, such prenatal intervention would be non-invasive, without significant maternal and foetal adverse effects[10]. Treprostinil is a non-teratogenic prostacyclin-analogue used to treat PH in neonates with CDH[11–14]. In vitro, treprostinil reduces the proliferation of pulmonary arteriolar smooth muscle cells[15–17]. In vivo, we previously demonstrated that in rat pups with nitrofen-induced CDH, transplacental treprostinil reduces the proportional medial wall thickness characteristic of pulmonary arterioles in CDH-PH[2]. In anticipation of clinical translation, the safety and efficacy of treprostinil must be validated in a larger animal model. In this study, we aimed to assess tolerance and effectiveness of prenatal treprostinil in rabbit pups with surgically-induced CDH.

2. Material and methods

2.1. Ethics

This study was approved by the Ethics Committee for Animal Experimentation of the KU Leuven of the Faculty of Medicine (P079/2021) and followed the ARRIVE 2.0 guidelines for reporting on animal research[18].

2.2. Animals

Time-dated, drug-naive pregnant rabbits (hybrid of New Zealand and Flemish Giant rabbits) were obtained from a registered breeder and housed in individual cages at 21 °C and 42% humidity, with a 12-hour day/night cycle and free access to water and food.

2.3. Treprostinil administration

To ensure continuous, subcutaneous administration of treprostinil (10 mg/mL Remodulin®, United Therapeutics Corporation, Silver Springs, MD, USA) programmable iPRECIO drug infusion pumps (SMP-200, Primetech Corporation, Tokyo, Japan) were used. Weight-adjusted treprostinil doses were prepared, using the formulas in the product data sheet[13]. Under sterile conditions, treprostinil was dissolved in

phosphate-buffered saline (PBS) 1X (Gibco, Thermo Fisher Scientific, Waltham, MA, USA) and loaded in the pump. In CTRL rabbits, a pump delivering NaCl 0.9% was implanted. Pumps were programmed to start drug delivery ten hours after surgical implantation, and 24 h when combined with CDH creation, to allow for post-anaesthesia recovery. Pumps were retrieved at the end of the experiment, thoroughly washed, programmed to pump sterile PBS through the catheter during 24 h, sterilized (2% glutaraldehyde for 12 h) and stored in a Penicillin/Streptomycin (100 U/mL, 100 µg/mL) solution until next use, as previously described[19]. Pumps were not re-used more than three times.

2.4. Pump implantation procedure

Pumps were implanted subcutaneously in the maternal neck scruff under general inhalation anesthesia (4% Sevoflurane, 2 L/min O₂). Since treprostinil can cause local erythema, care was taken to make a large subcutaneous pocket and to turn the tip of the drug delivery catheter away from the incision, prior to closure with intradermal resorbable sutures (Monocryl 3–0, Ethicon, Raritan, NJ, USA). In does undergoing surgical creation of CDH, pumps were implanted at the end of the procedure.

2.5. Treprostinil plasma concentration analysis

Maternal blood was sampled via cardiac puncture immediately prior to euthanasia, and fetal blood via decapitation. Blood samples were kept in EDTA tubes and centrifuged at 2000 g, 4 °C for 15 min. The supernatant plasma was collected and stored at – 80 °C for concentration analysis with validated ultra-high performance liquid chromatography-tandem mass-spectrometry (UHPLC-MS) analysis in two batches by the Laboratory of Pharmacology and Toxicology (Good Laboratory Practice compliant laboratory) at the Department Pathobiology, Pharmacology and Zoological Medicine at the Faculty of Veterinary Medicine of Ghent University in Merelbeke, Belgium. The methodology for the UHPLC-MS analysis is detailed in the [supporting information \(SI1\)](#). The transplacental transfer ratio was calculated as follows: [(average fetal concentration/average maternal concentration)*100] [2].

2.6. Maternal tolerance outcomes

From GD22 onwards, does were monitored daily for food intake (maximum 130 g/day), heart rate using electrocardiography (average of three sequential measurements), maternal weight and relative weight gain per pup calculated as $[body\ weight\ after\ therapy - body\ weight\ before\ therapy] / size\ of\ the\ litter$, pain using the validated rabbit grimace score [20] and behavior using a behavioral assessment scale ([Table S1](#)) [20–22]. Does were also inspected for treprostinil-specific adverse effects such as pump-site erythema, induration and/or edema, and finally acral redness and flushing[23].

2.7. Creation of diaphragmatic hernia

On GD23, does underwent surgery under general anesthesia for induction of a left-sided diaphragmatic defect as previously described (further referred to as congenital diaphragmatic hernia, CDH)[9,21,24]. The anesthesia protocol and surgical procedure is detailed in [supporting information \(SI2\)](#). Briefly, the surgical procedure consisted of a lower-midline laparotomy followed by sequential hysterotomy and fetal thoracotomy to eventually excise a portion of the left diaphragm. This was done in maximum five fetuses per doe, based on the litter size and whether the total operating time could be kept under 1h15. After the surgery, does were returned to their cages with free access to water and food, and monitored daily for pain.

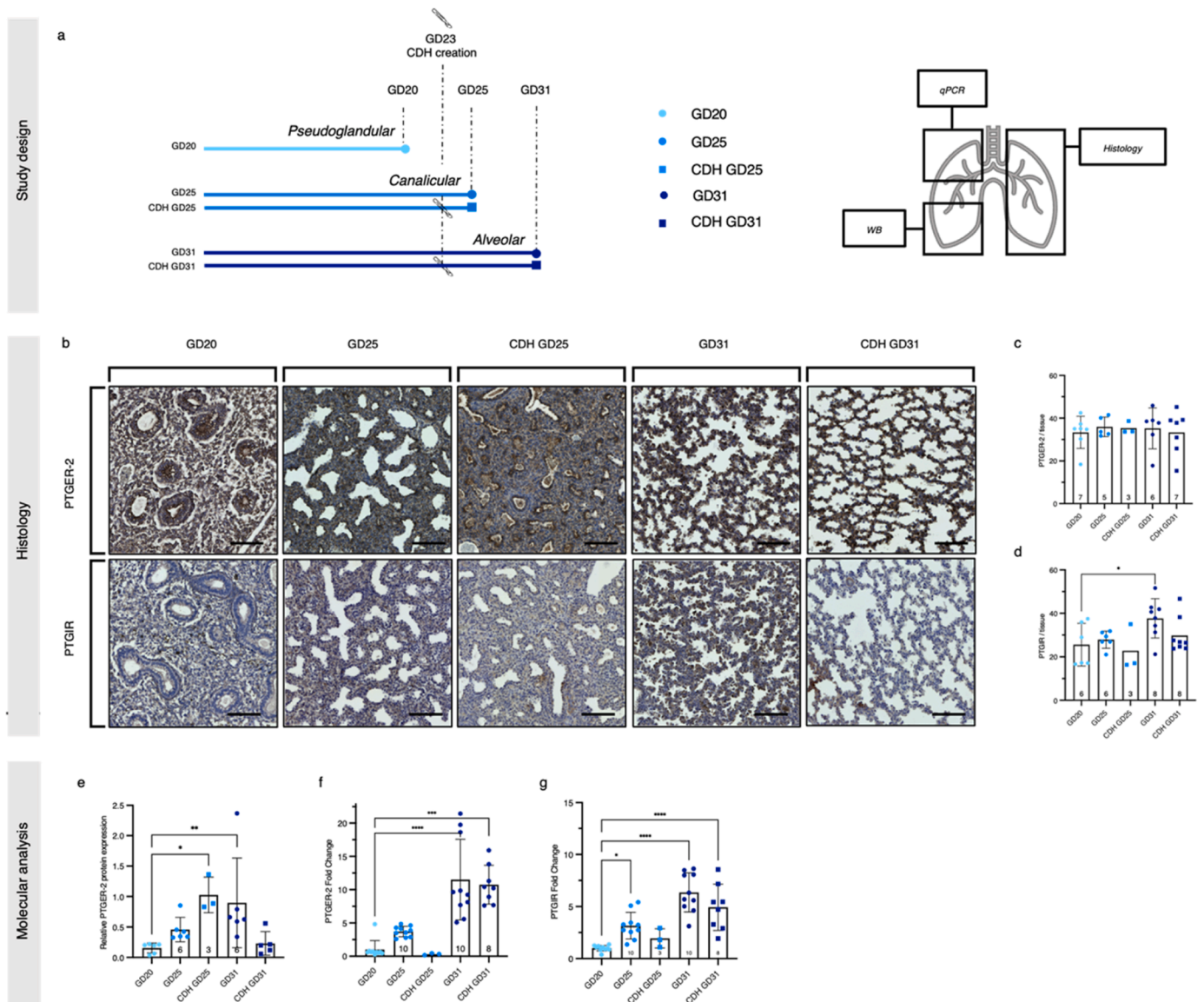


Fig. 1. Spatio-temporal expression of PTGER-2 and PTGIR. **a** Spatio-temporal study design, colour legend and lung processing. The scalpel icon represents the induction of CDH at GD23 in this surgical model. **b** Representative images of PTGER-2 and PTGIR expression in lungs of foetuses at *pseudoglandular* (GD20), *canalicular* (GD25) and *alveolar* (GD31) lung developmental phases. Scale bars represent 100 μ m. **c,d** Immunohistochemical PTGER-2 and PTGIR expression quantification relative to the total detected pulmonary tissue (%). **e** Relative pulmonary expression of PTGER-2 quantified with WB. **f,g** Pulmonary mRNA expression of PTGER-2 and PTGIR determined with qPCR. * = $p < 0.05$, ** = $p < 0.01$, *** = $p < 0.001$, **** = $p < 0.0001$.

2.8. Delivery and euthanasia

At term (GD31), does were sedated with intramuscular (IM) ketamine (0.5 mg/g, Nimatek®, Eurovet Animal Health BV, Bladel, The Netherlands) and xylazine (0.1 mg/g, XYL-M®, VMD, Arendonk, Belgium), followed by gas anesthesia using isoflurane (1.5%, ISO-VET®, Piramal Critical Care, Voorschoten, The Netherlands). After local infiltration of lidocaine (4 mg/kg, Xylocaine®, Aspen, Dublin, Ireland) a laparotomy and hysterotomy were performed to deliver the pups. All pups were weighed and either sedated with an intraperitoneal injection of ketamine (35 mg/kg, Nimatek®) to undergo mechanical ventilation or transcardial perfusion, or were immediately decapitated with sharp scissors to harvest the organs in a fetal state, prior to the first breaths. After delivery of the last pup, does were euthanized using IV 140 mg/kg pentobarbital (Euthasol®, Dechra, Bladel, The Netherlands).

2.9. Tissue harvest

For the spatio-temporal receptor expression study, unventilated lungs were divided. Left lungs were immersed in 4% paraformaldehyde (PFA) in 0.1 mol/L phosphate buffer (Klinipath®, Sowinskiego, Poland) with pH 7.4, whereas right lungs were snap frozen in liquid nitrogen and stored in baked aluminium foil for molecular analysis.

For the dose-finding and tolerance study, four pups per litter underwent transcardial perfusion for neuropathological examination (technique detailed in [supporting information \(SI3\)](#)). In the remaining pups, blood was collected via decapitation and hearts, left kidneys and placentas harvested and submersed in 4% paraformaldehyde (PFA). The lungs were dissected ‘en bloc’ and an angiocatheter (18–20 G) secured in the trachea. After tying off the right main stem bronchus, PFA was instilled in the left lung at a distending pressure of 20 cmH₂O during at least three hours. Right lungs were snap frozen with liquid nitrogen and stored in baked aluminum foil for molecular analysis. After euthanasia,

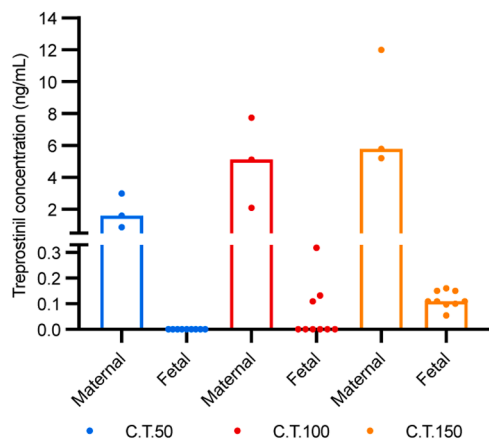


Fig. 2. Maternal and foetal treprostinil concentrations. Treprostinil concentrations were measured in does with term pups exposed to eight days of treprostinil at different doses 50 (C.T.50), 100 (C.T.100) or 150 (C.T.150) ng/kg/min. N = 3 does per dose, with three foetuses per litter. Bars represent median concentrations. The lower limit of quantification was 0.025 ng/mL.

ribs were manually counted in all pups of the litter.

For the efficacy study, litters were either dedicated to pulmonary function testing or fetal organ and lung harvest, as described for the dose-finding and tolerance study section. In operated pups, the presence of CDH was visually confirmed upon dissection.

2.10. Histology

Organs harvested for histology remained immersed in PFA during 48 h whereupon their volumes were determined using the fluid displacement method[25]. Organs were then transferred to ethanol (70%), dehydrated (70% ethanol, 90% ethanol, 99% ethanol, toluol), embedded in paraffin, sectioned coronally, stained and analyzed in an organ-specific manner as detailed below. Histological slides were digitized using a Zeiss AxioScan Z1 (AxioScan Slide Scanner, Carl Zeiss MicroImaging GmbH, Munich, Germany) and analyzed blinded to the study group.

Lungs were stained with hematoxylin and eosin (H&E), or with antibodies α -smooth muscle actin (α -SMA, mouse anti-human, M0851; DakoCytomation, Glostrup, Denmark), prostaglandin E2 receptor (ab167171, Abcam, rabbit monoclonal EPR8030B) or prostacyclin receptor (GTX71509, GeneTex, Irvine, CA, USA) (validation detailed in Fig. S3.). Horseradish peroxidase (ab2338503, goat anti-mouse, and ab2313567, goat anti-rabbit, polyclonal, Jacksonimmuno) was used as secondary antibody. Airway morphometry was assessed in 10–35 (depending on the lung size) randomly selected tiles per lung (500 × 500 μ m), using a validated semi-automated ImageJ analysis tool quantifying alveolar septal volume density (Vvsep), alveolar mean linear intercept (Lm), mean transsectional wall length (Lmw) and alveolar surface area density (Svair)[26]. Alveolar mean linear intercept (Lma) and alveolar surface area (S) were calculated using the methodology put forth by the American thoracic society[27]. Vascular morphometry was performed manually on slides stained with α -SMA, using the ZEN Microscopy Software (Zen Blue, Carl Zeiss, Oberkochen, Germany). Pulmonary arterioles were distinguished from pulmonary veins based on position and

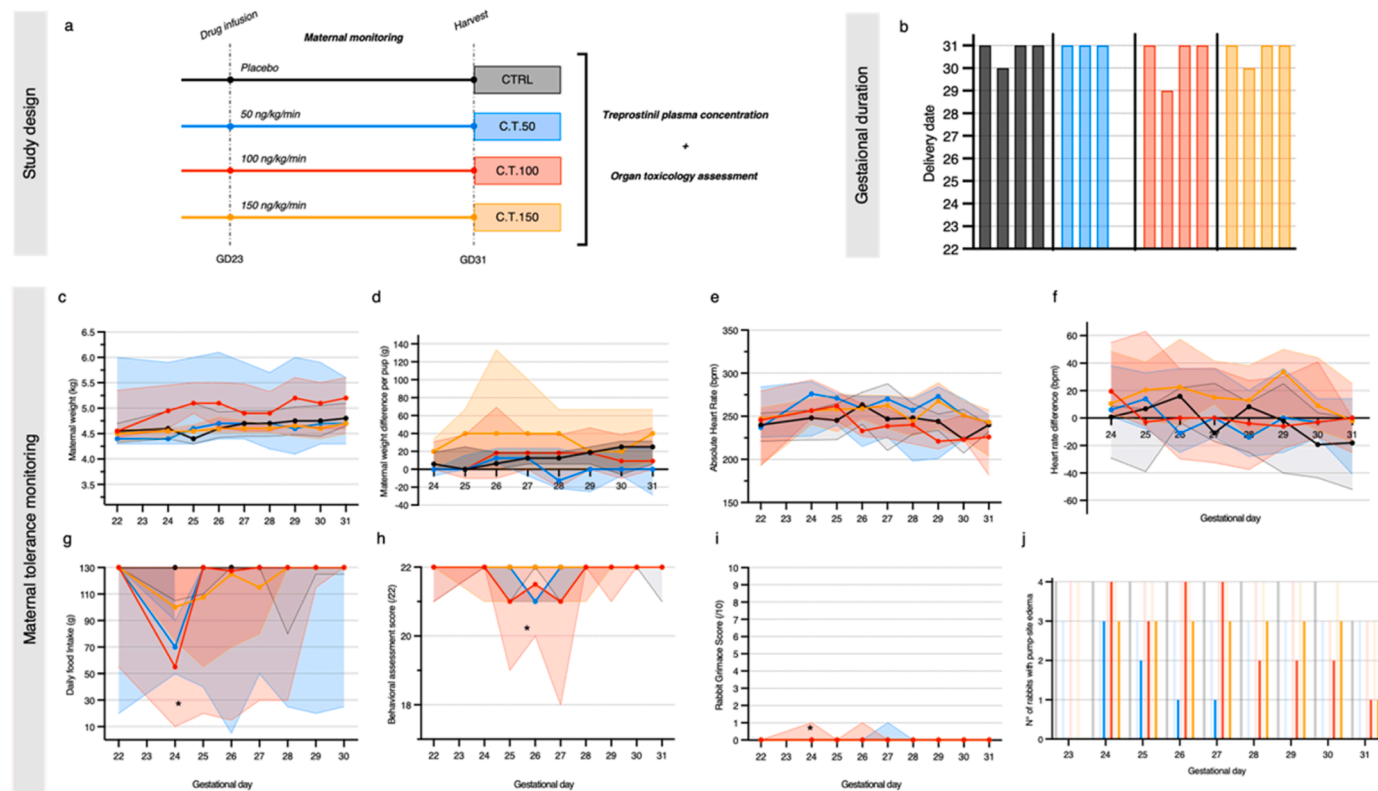
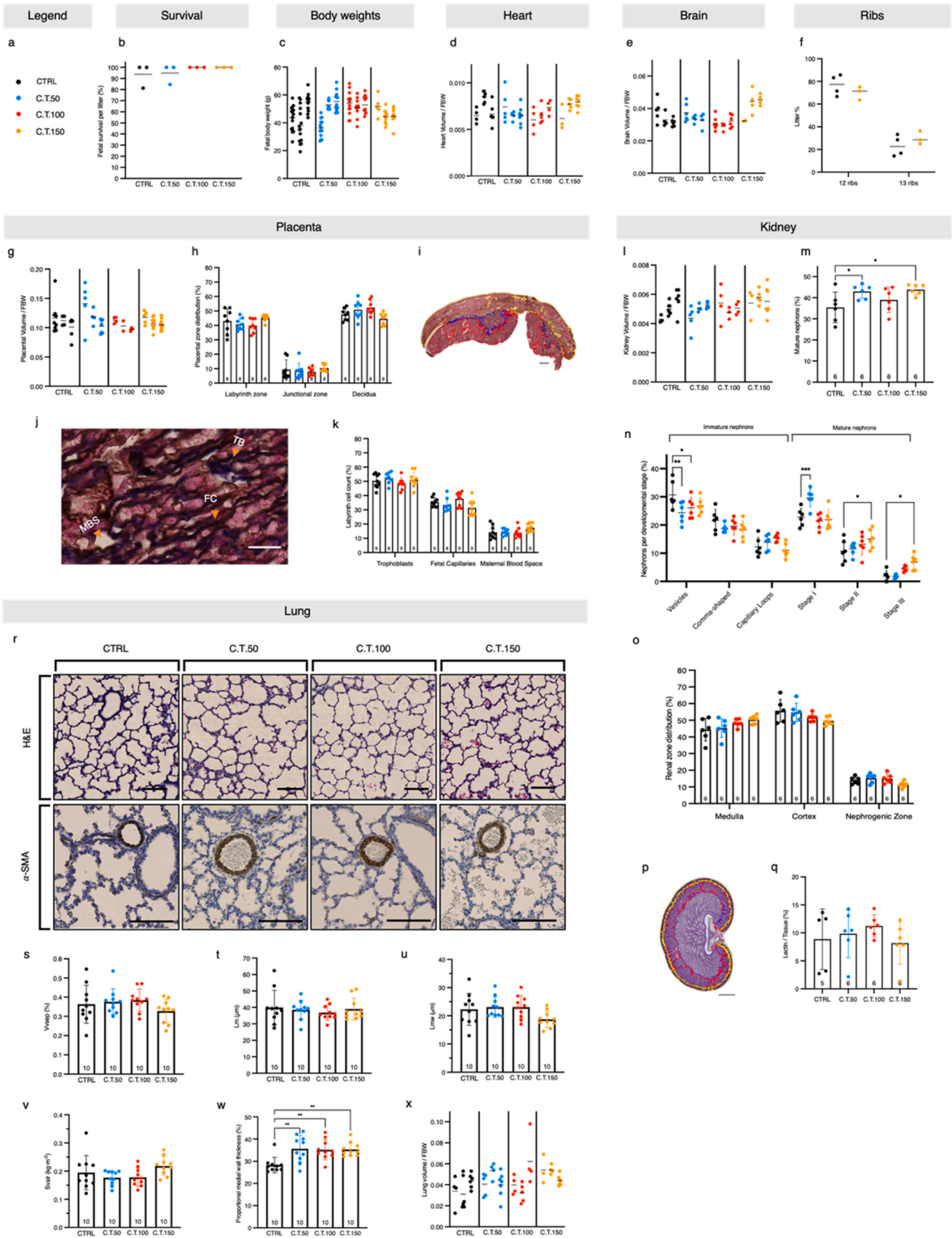


Fig. 3. Maternal tolerance. a Tolerance study design and colour legend. b Delivery date per group. c Maternal weight over time (kg). d Maternal weight change over time relative to baseline weight (weight t_x – weight t_{GD23}), corrected for litter size. e Daily maternal heart rate in beats per minute (bpm). f Change in maternal heart rate relative to baseline (heart rate t_x – heart rate t_{GD23}). g Daily food intake (grams). h Behavioural assessment scores (/22) over time. i Daily rabbit grimace score (/10). j Pump-site oedema over time. Transparent bars represent the number of does at given GD. Solid bars represent does with oedema at the pump-site per group. For graphs 3c-f: full lines represent medians, and dotted lines the interquartile range. For graphs 3 g-j: full lines represent medians, and dotted lines the range. Number of does per group were CTRL (n = 4), C.T.50 (n = 3), C.T.100 (n = 4) & C.T.150 (n = 4). * The C.T.100 rabbit with poor behavioural and grimace scores, also ate less and ultimately delivered prematurely on GD29.



(caption on next page)

Fig. 4. Foetal safety. Only pups from term litters were analysed. a Colour legend. b Foetal survival per litter (%). c Foetal body weight (FBW) in grams, nested per litter. d Heart volume/FBW ratio, nested per litter. e Brain volume/FBW ratio, nested per litter. f Percentage of pups per litter with 12 or 13 pairs of ribs counted. g Placental volume/FBW ratio, nested per litter. h Proportional distribution of surface area per placental zone (%). i Representative image of a cytokeratin/lectin-stained placental section with zone-surface areas delineated: the *decidua* in yellow, *junctional zone* in blue and the *labyrinth* in red. The scale bar represents 1 mm. j Representative histological image of the placental *labyrinth zone* stained with cytokeratin and lectin. *MBS* = maternal blood space, *FC* = foetal capillary and *TB* = trophoblast cell. White scale bar represents 40 μ m. k Proportional placental labyrinth cell count (%). l Kidney volume/FBW ratio, nested per litter. m Proportion of mature nephrons (%). n Proportion of nephrons per glomerular developmental stage (%). o Proportional renal zone surface area distribution (%). p Representative image of renal zone surface area distribution assessment on a H&E-stained section. The *nephrogenic zone* is delineated in yellow, the *cortex* in red and the *medulla* in blue. The scale bar represents 800 μ m. q Proportion of renal cortical tissue staining positively for lectin (%). r Representative images of pressure-fixed lungs stained with haematoxylin-eosin (H&E) and α -smooth muscle actin (α -SMA). Bars represent 100 μ m. s-v Airway morphometry; $V_{v,sep}$ = volume density of alveolar septa, L_m = mean linear intercept of airspaces, L_{mw} = mean transectional wall length and $S_{v,air}$ = surface area density of air spaces. w Proportional medial wall thickness of pulmonary arterioles. x Lung volume/ FBW ratio, nested per litter. *Full lines represent means and error lines represent standard deviations.* Number of foetal pups is indicated at the bottom of bar graphs. One-way ANOVA with Dunnett's multiple comparison test was performed with the CTRL group as reference (b,h,k,m-o,q,s,u,v and nested per litter: c,d,e,g,l,x). Kruskal-Wallis multiple comparison test with CTRL as reference was performed for L_m and %MWT (t,w). Student t-test was used to compare rib counts (f). * = $p < 0.05$, ** = $p < 0.01$, *** = $p < 0.001$.

structure. Only those pulmonary arterioles were considered that were approximately round (i.e. two perpendicularly measured internal diameters (ID) were not different > 50%) and the mean ID was $\leq 100 \mu$ m. The mean external diameter (ED) as well as mean ID were then measured, and the proportional medial wall thickness (%MWT), a surrogate maker of pulmonary hypertension, calculated as follows $\%MWT = [(ED-ID)/ED \times 100]$ [28]. Arterioles were further categorized in three groups according to the external diameter (ED); i.e. intra-acinar (ED < 30 μ m), ED between 30 and 60 μ m, and pre-acinar (ED 60–100 μ m). Quantification of Sirius Red, PTGER-2 and PTGIR stain was performed using custom ImageJ macros of which the code is provided in the [supporting information \(S14\)](#).

For cerebral histology, four serial coronal sections (thickness 4 μ m) were taken at 50 μ m intervals at the level of medial septal nucleus (for examination of the frontal cortex (FC) in the internal pyramidal layer and the caudate nucleus (CN)) and another four at the level of the hippocampal formation (for investigation of the hippocampal CA₃ region and the dentate gyrus (DG)) [29]. Sections were stained with Cresyl-Violet (Cresyl-Violet acetate, Sigma-Aldrich®, Darmstadt Germany) and for brightfield immunohistochemistry primary antibodies used were mouse monoclonal anti-human Ki67 (M724001–2, Agilent, Diegem, Belgium) for proliferation, *Glial Fibrillary Acidic Protein* (GFAP, G6171, Citeab, Bath, UK) for astrocytosis, *Neuron-Glial antigen 2* (NG2, AB5384-I, MerckMillipore, Burlington, MA, USA) for oligodendrocyte progenitor cells and biotinylated isolectin B4 (B-1205, Vector Laboratories, Burlingame, CA, USA) for microvascularisation [30]. The secondary antibody was goat anti-mouse peroxidase (115–035–044, Jackson ImmunoResearch®, Cambridgeshire, United Kingdom). Degenerating nuclei were visualized by the terminal deoxynucleotidyl transferase dUTP nick end labeling (TUNEL) method for fluorescent in situ end labeling of double-stranded DNA fragmentation (Apoptag S7110; Millipore). Sections were counterstained with Hoechst 33342 (Sigma-Aldrich) [29]. Histological quantification was performed in the FC, CN and the hippocampus, using the open-source QuPath (version 0.2.3, Centre for Cancer Research & Cell Biology, Queen's University Belfast, Belfast, Northern Ireland, Open source) [31] and ImageJ (Version 1.51 g, Fiji, USA) [32]. Per slide, three random squares (100 \times 100 μ m) were selected on low magnification: (1) in the internal pyramidal layer of the frontal cortex, (2) the caudate nucleus and (3) in the hippocampus CA₃ region. In the hippocampus, neurons were counted in the lateral 500 μ m of the dentate gyrus. Neuron density was counted manually on Cresyl-Violet-stained slides. Neuron densities were expressed as number of neurons per mm² or as number of neurons per mm in the dentate gyrus. Neuron densities were counted on three consecutive slides and their average was reported [30]. TUNEL, Ki67 and NG-2 positive cells were counted using the positive cell detection function in QuPath under either bright-field or fluorescent positive cell detection settings [29,30]. The detection classifier function was used to differentiate between cell types [31,33]. Positive cell counts were expressed as a percentage of positive cells per total cells detected.

Quantification of lectin and GFAP stain, were performed using custom ImageJ macros of which the code is provided in the [supporting information \(S15\)](#).

A coronal section through the middle of both placental lobes was stained with cytokeratin (nb600–579, Novus Biologicals; 1:75, overnight, 4 °C) and lectin (Isolectin B4, B-1205, Vector Laboratories; 1:250, 90 min, 37 °C), to differentiate cytotrophoblasts and fetal capillaries in the labyrinth zone respectively [34]. The proportion of fetal capillaries, maternal blood spaces and trophoblasts within the labyrinth was determined on ten random fields at 40x magnification using a 5 \times 2 point counting grid (100 points analyzed per placenta) [34]. Proportional surface areas of the labyrinth, decidua and junctional zone were measured using the QuPath wand tool.

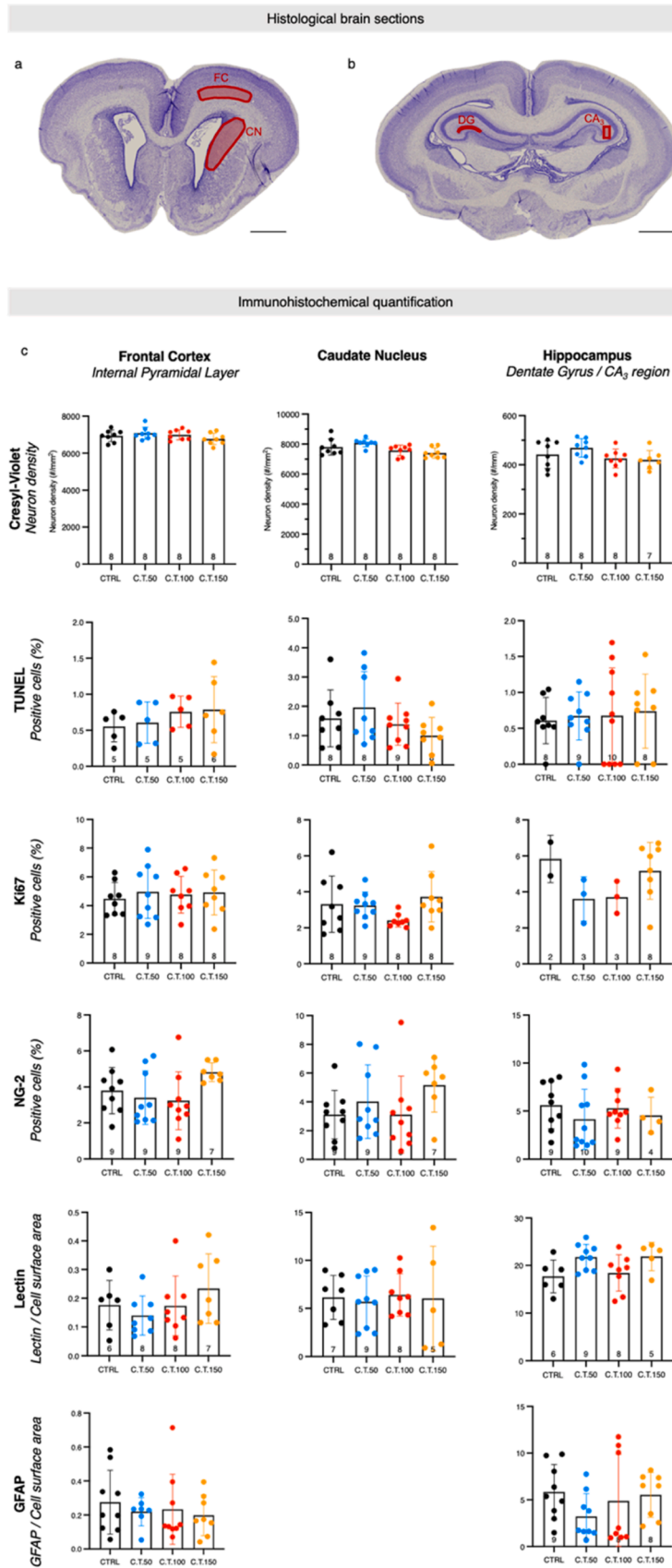
A coronal section through the middle of the renal pelvis was stained with H&E and biotinylated isolectin. Proportional surface area of medulla, cortex and nephrogenic zone were measured using the QuPath wand tool over the entire slide. Glomerular maturity was scored as previously described, in the upper, medial quadrant by two observers (FRDB & AD) [35].

2.11. Lung mechanics testing

Lung mechanics tests were performed using the FlexiVent 5.2 (SCIREQ, Montreal, Canada) on anesthetized neonatal pups from dedicated litters. A tracheotomy was performed to insert a 18 G metal cannula and start lung-recruitment breaths (RR: 120 breaths/min, tidal volume: 8 mL/kg, PEEP: 3 cmH₂O). Once the inspiratory capacity (IC) reached a plateau, triplicate measurements were obtained of a series of pulmonary function tests consisting of (1) an IC measurement, (2) a single-frequency oscillation (Snapshot 150: a single-frequency measurement at 2.5 Hz) to assess dynamic compliance (Crs), (3) a broadband oscillation maneuver (Primewave-8: measuring respiratory impedance from 0.5 Hz to 19.5 Hz) to assess tissue stiffness, and (4) pressure-volume maneuvers (PvR-P: continuous increase of airway pressure to 13 cmH₂O, Pvs-P: staged increase of airway pressure to 30 cmH₂O) [36], [37]. IC and Cst were corrected for weight. When system-detected errors could not be corrected or the ultimate IC was not > 50% higher than the first IC, pups were excluded from analysis.

2.12. Western blot

Tissue samples were mechanically homogenized in RIPA lysis buffer (10 mM sodium phosphate (pH 7.5), 150 mM NaCl, 1.5 mM MgCl₂, 0.5 mM DTT, 1% Triton X-100), with protease- and phosphatase inhibitors (11836153001, cOmplete™, Roche, Basel, Switzerland). Protein concentration was determined using a Pierce BCA Protein Assay Kit (23225, Thermo Fisher Scientific). Equal quantity (μ g) of samples was prepared with SDS buffer containing β -mercaptoethanol, heated at 95 °C for 3 min and 15 μ L loaded on NuPAGE 4–12% Bis-Tris gels (NP0321BOX, Thermo Fisher Scientific). SDS-PAGE was performed with a constant voltage of



(caption on next page)

Fig. 5. Cerebral morphometry. a Representative cerebral section through the frontal cortex (FC) and the caudate nucleus (CN). Measurements were performed in the internal pyramidal layer of the FC and the CN (zones marked in red). Scale bar represents 1 mm. b Representative cerebral section through the hippocampus. Measurements were performed in the dentated gyrus (DG) and CA₃ region of the hippocampus (zones marked in red). Scale bar represents 1 mm. c Quantified (immuno-) histochemical analysis per region. Cresyl-Violet was used for neuron density count in the FC, CN and DG. TUNEL-positive cells indicated apoptosis in the FC, CN and CA₃. Proliferation was assessed by means of positive Ki67 cell counts in the FC, CN and CA₃. Oligodendrocyte-progenitor cells were counted as NG-2 positive cells in the FC, NC and CA₃. Lectin surface area was quantified and expressed in proportion to the total cell surface area in the FC, CN and CA₃. Astrocytosis was assessed quantifying the surface area of GFAP expressed in proportion to the total cell surface area in the FC and CA₃. Full lines represent means and error lines represent standard deviations. Number of fetal pups was indicated at the bottom of bar graphs. Data were compared using Dunnett's multiple comparison test with the control group as reference.

160 V during one hour. Next, proteins were blotted on polyvinylidene difluoride (PVDF) transfer membranes (88518, Thermo Fisher Scientific) using the Mini Blot module set (B1000, Thermo Fisher Scientific) for two hours at 30 V. Membranes were blocked for one hour at room temperature with PBS-Tween (0.1%) containing 5% milk powder (MP) followed by incubation with the PTGER-2 primary antibody (ab167171, Abcam, Cambridge, UK) diluted in PBS-T and 2% MP overnight at 4 °C. Next day, the membranes were washed three times with PBS-T and then incubated with the secondary horseradish peroxidase (HRP)-coupled antibody (P044801-2, goat anti-rabbit, Agilent) for 45 min with PBS-T + 2%MP. After washing three times with PBS-T, immunoreactive bands were visualized through enhanced chemoluminescence (Pierce ECL Plus Western Blotting Substrate, SuperSignal West Dura, 34075, Thermo Fisher Scientific), followed by serial exposure and detection with the G: Box GelDoc system from Syngene (Cambridge, UK). Intensity quantification was performed on unsaturated bands with ImageJ[38].

2.13. Quantitative polymerase chain reaction

mRNA was extracted using the Tri-Pure® Isolation reagent (Roche Diagnostics, Germany) and its concentration measured using the Nanodrop 1000® spectrophotometer (Thermo Fisher Scientific). Agarose gel electrophoresis was used to verify RNA integrity (integrity of 18 S and 28 S bands). TaqMan™ Reverse Transcription Reagents (Thermo Fisher Scientific) was used for cDNA synthesis. For detection the Platinum SYBR Green qPCR Supermix-UDG with ROX (Thermo Fisher Scientific) was used. YWHAZ was used as stable housekeeping gene to normalize mRNA levels. The primers were obtained from Integrated DNA Technologies (Haasrode, Belgium) and are detailed in Table S2. Samples were run in triplicate on a StepOne Plus® instrument (Thermo Fisher Scientific). Relative quantitation was determined using the comparative Ct method. Statistics are calculated in based on $\Delta\Delta C_t$ values, while fold change (FC) was used for visualization[36],[39].

2.14. Enzyme-linked immune-sorbent assay (ELISA)

Tissue samples were mechanically homogenized in RIPA lysis buffer containing Tris-HCL and EDTA. Cyclic adenosine monophosphate (cAMP) was quantified using a commercial ELISA kit (MBS2600879, Mybiosource.com, San Diego, CA, USA) according to the manufacturer's protocol.

2.15. RNA sequencing

Total RNA was extracted using the RNeasy mini kit (Qiagen, Hilden, Germany) according to the manufacturer's instructions. Initial quality control was performed using the Bioanalyzer 6000 Nano. Sequencing was performed by Azenta (Azenta Life Sciences, Griesheim, Germany). The methodology is detailed in the supporting information (SI6). The Illumina NovaSeq platform was used on poly-A selected mRNA with 2 × 150 pair-end reads. Trimmed reads (Trimmomatic v.0.36.) were mapped on the rabbit reference genome (OryCun2.0) using STAR aligner v.2.5.2b. Differential gene expression was performed using R-studio (2022.12.0) with the DESeq2 library[40]. We included genes with a count per million greater than 1 in at least two samples. Significant differential gene expression was determined using an adjusted p-value

less than 0.05 and a log₂ fold change (log₂FC) greater than 1 or less than - 1 as cut-offs.

2.16. Sample size

For the receptor and tolerance study no power calculation was performed. For the dose-finding study, three does per group were used as is customary for maternofetal pharmacokinetic studies[21]. For the efficacy study, based on previous studies[21,41] we determined using G*Power[42], that 6–7 fetuses/group would provide a power of $\geq 90\%$ with a two-sided type I error of 5%, to detect a 10% reduction in %MWT (primary study outcome).

2.17. Statistics

The Shapiro-Wilk test was used to assess the distribution of variables. Normally distributed values were expressed as means \pm standard deviations and analysed with t-test or one-way analysis of variance (ANOVA) with Dunnett's multiple comparison test to assess differences between groups. Non-normally distributed values were presented as medians and interquartile ranges and analysed using the Kruskal-Wallis test with multiple comparisons testing. Organ and foetal body weights were analysed using nested analysis to correct for litter-specific influences. A complete overview of outcome measures, their distribution, the statistical tests used and the F (ANOVA) and t-values (t-tests) with degrees of freedom are provided in Table S3. Significance was determined as $p < 0.05$. Data was analyzed using Prism version (GraphPad, San Diego, CA, USA).

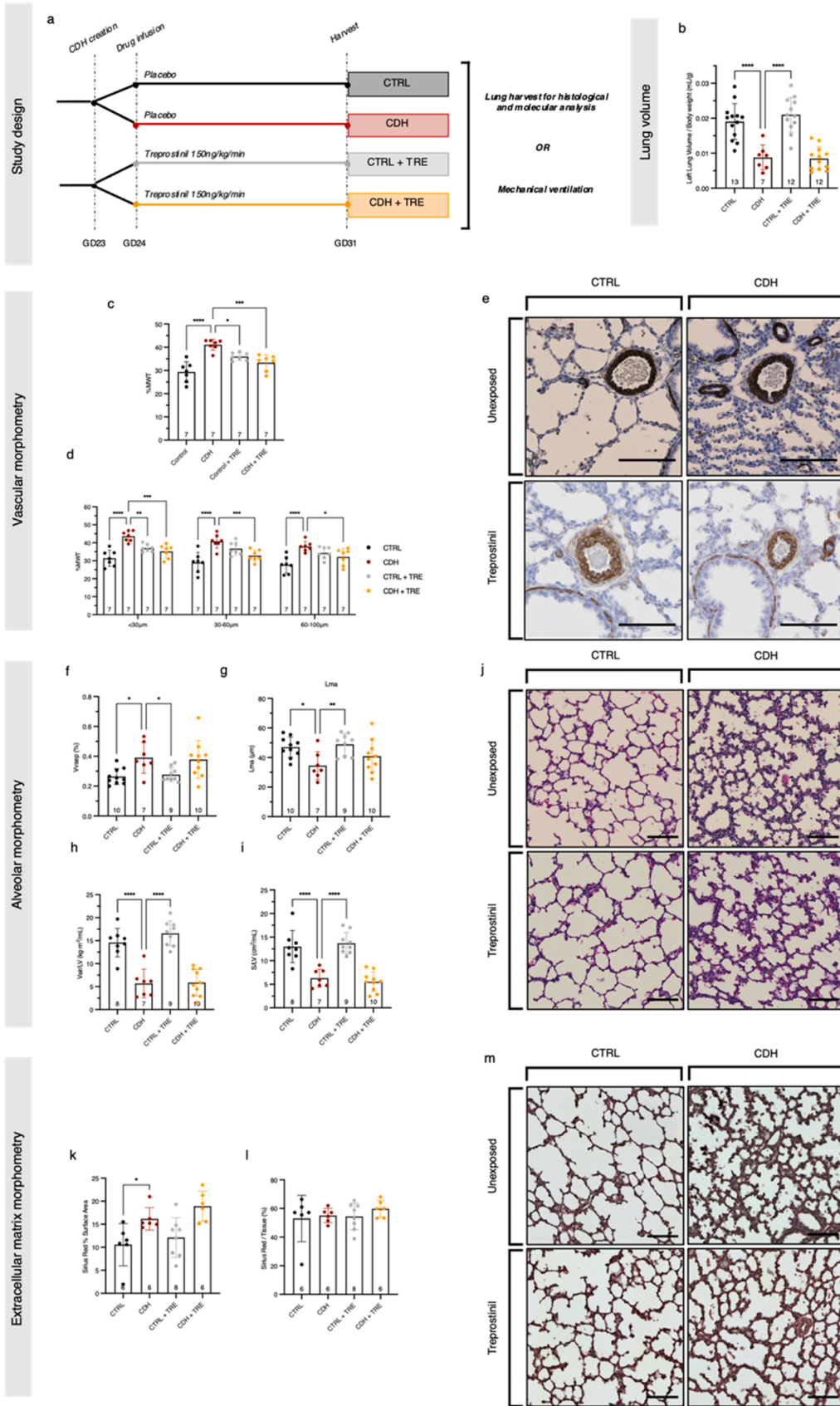
3. Results

3.1. Pulmonary PTGER-2 and PTGIR expression progressively increase throughout gestation

We first mapped the spatio-temporal pulmonary expression of the two receptors that mediate treprostinil's antiremodeling effect, i.e. prostaglandin E₂ (PTGER-2) and prostacyclin (PTGIR)[17,43]. Lungs of unoperated pups and pups with CDH were harvested at the following gestational ages, each representative of a specific lung developmental stage: gestational day (GD) 20 pseudoglandular, GD25 canalicular, and GD31 (=term) alveolar (Fig. 1a)[44]. Receptor expression was assessed by immunohistochemistry and quantified with quantitative polymerase chain reaction (qPCR) and western blotting (WB). PTGER-2 and PTGIR were primarily expressed in the respiratory epithelium and pulmonary arterioles (Fig. 1b & Fig. S1.). Quantification of PTGER-2 and of PTGIR expression per lung tissue area demonstrated respectively stable and increasing ratios over lung developmental stages in unoperated pups (Fig. 1c,d). PTGER-2 protein expression increased with gestation in lungs of unoperated pups, however, was markedly lower in term pups with CDH (Fig. 1e). mRNA expression for both receptors gradually increased over gestation both for lungs of control and CDH pups (Fig. 1f, g).

3.2. Treprostinil crosses the placenta

Next, we sought to investigate transplacental transfer of continuous



(caption on next page)

Fig. 6. Lung morphometry. a Efficacy study design, colour legend and lung assessment. b Left lung volume to foetal body weight ratio (mL/g). c Proportional medial wall thickness (%MWT) of resistance vasculature i.e. pulmonary arterioles with an internal diameter < 100 μ m. d %MWT per vessels size (external diameter (ED) < 30 μ m or intra-acinar arterioles, ED between 30 and 60 μ m, and ED 60–100 μ m or pre-acinar arterioles). e Representative images of pulmonary arterioles in pressure-fixed lungs stained with α -smooth muscle actine (α -SMA). f-i Quantified pulmonary alveolar morphometry; V_{vsep} = volume density of alveolar septa (%), L_{ma} = mean linear intercept of parenchymal airspaces, V_{air}/LV = Air space volume relative to left lung volume and S/LV = Alveolar surface area relative to left lung volume. j Representative images of pressure-fixed lungs stained with haematoxylin-eosin (H&E). k&l Collagen quantification with Sirius Red stain, expressed per surface area (%) and expressed per tissue surface area respectively (%). m Representative images of pressure-fixed lungs stained with Sirius Red. Full lines represent medians, and dotted lines the range. Data were compared using Dunnett's multiple comparison test with the CDH group as reference. Bars represent 100 μ m. * = $p < 0.05$, ** = $p < 0.01$, *** = $p < 0.001$, **** = $p < 0.0001$.

subcutaneous maternal administration of treprostinil. Programmable drug infusion pumps were implanted in the maternal neck scruff on GD23. At term (GD31), blood was collected from does and foetuses for treprostinil plasma concentration determination using ultra high-performance liquid chromatography-tandem mass spectrometry (UHPLC-MS). Examined doses were determined based on toxicology experiments in pregnant rabbits as part of treprostinil's New Drug Application (NDA) at the Food and Drug Administration. Since these studies reported maternal side effects (reduction in food intake and body weight) at a dose of 150 ng/kg/min, we used 50 (Control-Treprostinil 50, C.T.50), 100 (C.T.100) and 150 ng/kg/min (C.T.150) [23]. Maternal and fetal concentrations were dose-dependent (Fig. 2), with only the highest dose (150 ng/kg/min) consistently attaining fetal concentrations above the lower limit of quantification (0.025 ng/mL) with an average transplacental transfer ratio of 1.66% (\pm 0.61%).

3.3. Treprostinil is tolerated by does and increases glomerular maturation and pulmonary arteriolar hypermuscularization in foetal pups

In parallel to the pharmacokinetics, we assessed maternal tolerance and foetal safety in unoperated animals exposed to treprostinil at 50, 100 and 150 ng/kg/min as compared to placebo (NaCl 0.9%, CTRL group). Three term-delivered litters were obtained per group. Maternal heart rate, weight, food intake, pain, behaviour, and pump site were assessed daily, starting one day prior to the pump implantation (GD22) until delivery at term (Fig. 3a). Three does spontaneously delivered preterm: one in the CTRL (GD30), one in the C.T.100 (GD29) and one in the C.T.150 group (GD30) (Fig. 3b). Maternal weight gain and heart rate did not differ in treated groups compared to unexposed controls (Fig. 3c-f). After pump implantation, does receiving treprostinil had a temporary (one day) reduction in food intake, regardless of the dose (Fig. 3g). In two does (C.T.50 & C.T.100), food intake remained lower for the remainder of the pregnancy. Maternal behavioural and pain scores were not different in treprostinil-exposed groups from those in the unexposed controls. Oedema at the pump-site was noted day one after implantation in almost all does exposed to treprostinil, regardless of the dose, however not in the CTRL group. In does receiving 50 ng/kg/min treprostinil, oedema regressed over the course of four days. In does with 100 and 150 ng/kg/min oedema persisted longer (Fig. 3j).

Only foetuses from term litters were analysed. Foetal survival and body weight were not different among groups (Fig. 4b,c). The volumes of hearts, brains, placentas, left kidneys and lungs relative to body weight from treprostinil-exposed foetuses did not differ from controls (Fig. 4d,e,g,l,x). The anatomical variation of an additional 13th rib was equally prevalent in C.T.150 and CTRL groups (Fig. 4f). No morphological differences were observed between placentas from different groups (Fig. 4h-k). Alveolar septal thickness, septal volume and surface area density were not altered by treprostinil administration (Fig. 4l-o). Interestingly, pulmonary arteriolar proportional smooth muscle wall thickness (%MWT) was increased in treprostinil-exposed foetuses independent of the dose (Fig. 4r,w). There was no change in the ratio of renal cortex, medulla, and nephrogenic zones, or renal cortical vascularity in foetuses exposed to treprostinil, however the proportion of mature nephrons was higher (Fig. 4m-q). Cerebral immunohistochemical analysis revealed no measurable effects on neuron density, apoptotic cell count, cellular proliferation, oligodendrocyte progenitor

cells density, microvascularization and astrocytosis in foetuses exposed to treprostinil (Fig. 5c).

3.4. Treprostinil reduces pulmonary arteriolar hypermuscularization in term CDH pups

Having demonstrated consistent foetal-maternal transfer and acceptable maternal and foetal tolerance of 150 ng/kg/min treprostinil, we investigated its effects in rabbit foetuses with CDH. On GD23, CDH was surgically created in selected pups, and does were exposed to either saline solution (CDH group) or treprostinil (CDH+TRE group) using a subcutaneous pump placed in the maternal neck scruff. Infusion was programmed to start 24 h after implantation until caesarean section at term (Fig. 6a). Unoperated littermates constituted the controls, either exposed to treprostinil (CTRL+TRE group) or not (CTRL group). As expected, pups with CDH displayed a higher pulmonary arteriolar % MWT than CTRL ($41.1 \pm 2.3\%$ vs $29.3 \pm 4.4\%$, $p < 0.0001$). The %MWT in the CDH+TRE group was significantly lower than in placebo-exposed CDH ($33.4 \pm 3.4\%$ vs $41.1 \pm 2.3\%$, $p = 0.0003$) in all vessels < 100 μ m, and most pronounced in the smaller-sized vessels (<30 μ m) (Fig. 6d). % MWT was increased in CTRL+TRE pups relative to CTRL ($36.0 \pm 1.7\%$ vs $29.3 \pm 4.4\%$, $p = 0.0016$) (Fig. 6c-e).

3.5. Lung hypoplasia, airway and extracellular matrix morphometry in pups with CDH remain unchanged following treprostinil exposure

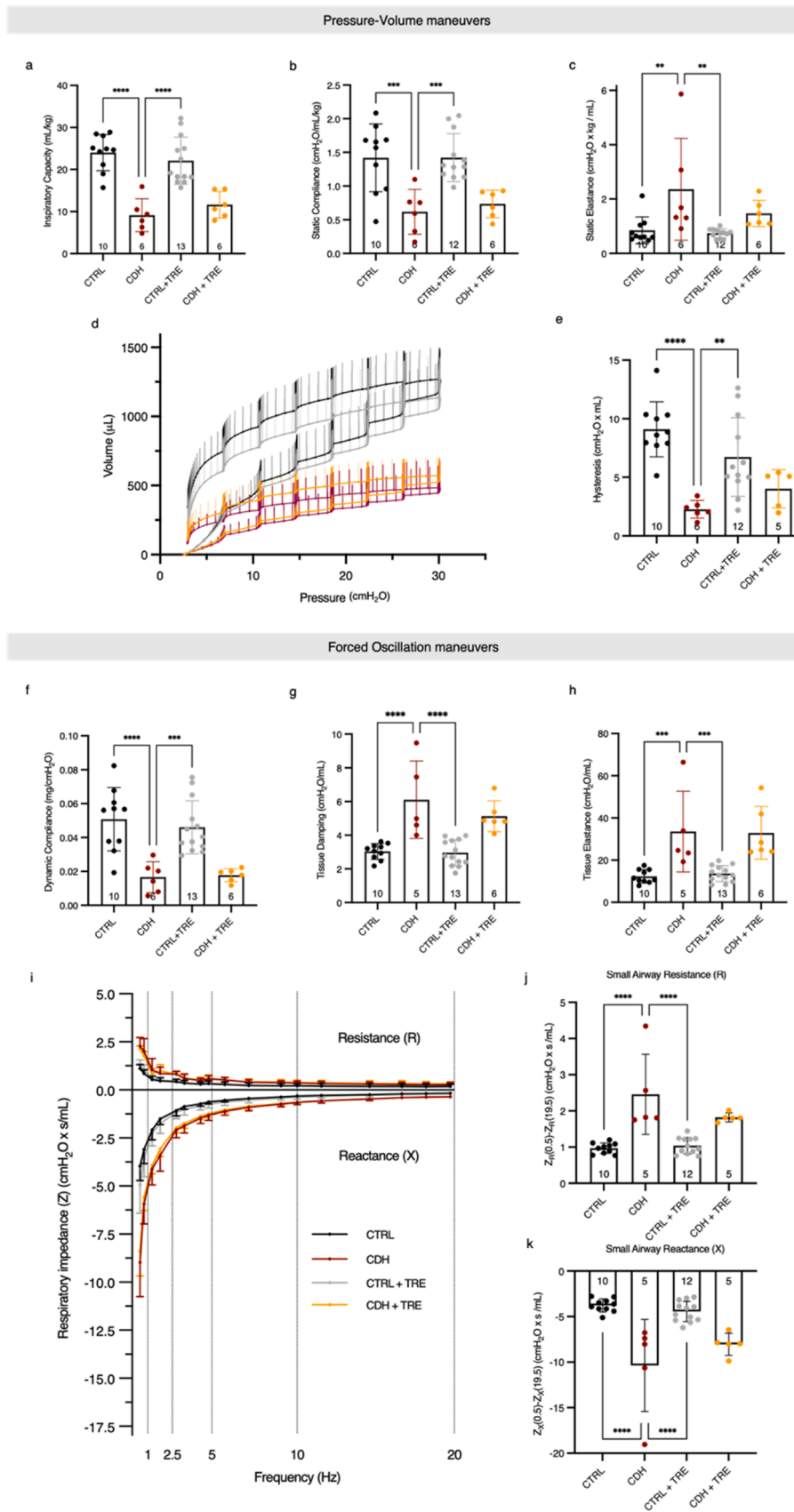
Ipsilateral, left lung volumes relative to foetal body weights were lower in pups with CDH, regardless of treprostinil exposure (Fig. 6b). Alveolar septal density (V_{vsep}) was higher in CDH than CTRL pups and not different after prenatal treprostinil exposure. Similarly, alveolar mean linear intercept (L_{ma}), volume (V_{air}/LV) and surface area relative to the left lung volume (S/LV) were impaired in CDH, and not altered with treprostinil exposure (Fig. 6f-j). Airway morphometry was not different between CTRL and CTRL+TRE groups. Quantification of Sirius Red stain suggested comparable collagen I and III deposition when expressed proportional to total tissue area (Fig. 6k-m).

3.6. Treprostinil does not improve pulmonary mechanics in CDH

A dedicated subset of pups from all four groups were ventilated immediately after birth for invasive lung mechanics assessment. Lung mechanics parameters both during pressure-volume and forced oscillation manoeuvres were significantly different in pups with CDH compared to CTRL, and similar observations were made in treprostinil-exposed pups. In pups without CDH, treprostinil administration did not affect pulmonary mechanics (Fig. 7).

3.7. Treprostinil downregulates inflammation, coagulation and myogenesis in CDH without affecting receptor expression

To characterize the mechanism of action of treprostinil on pulmonary vascular development, we performed RNA sequencing on unventilated left lungs lobes of CDH, CDH+TRE and CTRL pups ($n = 2-3$ /group). We observed a positive enrichment of interferon alpha and gamma in lungs of pups with CDH compared to CTRL (Fig. S2). Principal component analysis revealed clustering of CDH + TRE separate from



(caption on next page)

Fig. 7. Pulmonary function testing. Testing consisted of pressure-volume manoeuvres which generated: a Inspiratory capacity (mL/kg). b Static compliance (cmH₂O/mL/kg). c Static elastance (cmH₂O x kg / mL). d Pressure-volume curves plotted as averages per group with error bars depicting the standard deviation. e Hysteresis (cmH₂O x mL). Forced oscillation manoeuvres were performed generating: f Dynamic compliance (mg/cmH₂O). g Tissue damping (cmH₂O/mL). h Tissue elasticity (cmH₂O/mL). i Respiratory impedance (Z) (cmH₂O x s / mL) depicted as resistance (R) and reactance (X). j Calculated small airway resistance. k Calculated small airway reactance. Data were compared using Dunnett's multiple comparison test with the CDH group as reference. Bars represent 100 μ m. ** = $p < 0.01$, *** = $p < 0.001$, **** = $p < 0.0001$.

CDH, and together with CTRL in principle component 1 (Fig. 8a). Differential gene expression analysis using a cut-off value of $|\log_2$ fold change| > 1% and 5% FDR reveals 97 upregulated and 82 downregulated genes when comparing CTRL with CDH and 33 upregulated and 71 downregulated genes when comparing CDH versus CDH+TRE (Dataset S1&S2). Of the 97 upregulated genes in pups with CDH, 23 were downregulated when exposed to treprostinil (Fig. 8b, Dataset S3). We next performed gene set enrichment analysis of CDH versus CDH+TRE lungs using the hallmark gene set of the Molecular Signatures Database. We found significant enrichment (5% FDR) of 15 gene sets (Fig. 8c, Dataset S4&S5). Among those gene sets, we identified enrichment for genes downregulated in CDH+TRE pups related to coagulation, inflammatory response, complement activation, and myogenesis (Fig. 8c,d). These pathways correspond to the known mechanisms of action of treprostinil. Upregulation of mitochondrial transcripts and genes involved in the oxidative phosphorylation pathway was also observed in treprostinil treated pups with CDH (Fig. 8c,e).

Compared to CTRL, pulmonary PTGER-2 protein expression was not different in CDH pups, however, was increased in CTRL+TRE ($p = 0.0029$) (Fig. 9a). PTGER-2 mRNA expression was increased in CDH, however not altered by treprostinil (Fig. 9b). PTGIR and its synthase (PTGIS) were not consistently affected by CDH and/or treprostinil exposure (Fig. 9c,d). Cyclic adenosine monophosphate (cAMP), a key downstream regulator in the prostacyclin pathway was slightly higher in treprostinil-exposed pups, however this was not significant (Fig. 9e).

4. Discussion

We first demonstrated the expression of treprostinil's target receptors at relevant timepoints during gestation in control and CDH pups. Next, we quantified transplacental passage of maternal treprostinil into the foetal circulation without limiting adverse effects in does and foetuses at doses up to 150 ng/kg/min. Subsequently, in foetal rabbits with surgically created CDH, prenatal exposure to treprostinil (150 ng/kg/min) prevented the hallmark hypermuscularization of pulmonary arterioles (<100 μ m) and was associated with downregulated molecular pathways involved in inflammation, coagulation and myogenesis. No effect on airway morphometry and lung mechanics was observed. In foetuses with normal lung development, prenatal treprostinil exposure increased pulmonary arteriolar wall thickness.

We corroborated our previous findings in the nitrofen rat model in a larger model with lung development more similar to humans[2]. Unlike rodents, rabbits and humans undergo alveolarization in utero[41]. Surgical induction of CDH in rabbits during the pseudoglandular lung developmental phase reproduces the clinical phenotype in terms of pulmonary airway and vascular morphometry, as well as pulmonary function testing[24,45]. The rabbit model is also better suited for assessment of foetomaternal safety. Placental transfer in the latter half of pregnancy mirrors that in humans, since the rabbit mid- and end-gestational placenta is functionally positioned between rodents (hemo-trichorial) and humans (hemo-monochorial)[46–48]. Pregnancy-induced hemodynamic changes are also comparable with those in pregnant women, with an important increase in maternal blood pressure throughout gestation[46,47].

We first confirmed the presence of treprostinil's target receptors in lungs of healthy pups from the pseudo-glandular (GD20), and in CDH pups from the canalicular lung development phase (GD25) onwards through histological and molecular analysis. Corresponding with the

16th – 26th week of human gestation, the canalicular lung development phase occurs when CDH is most often diagnosed clinically (18–22 weeks GA) and represents the first window of opportunity for prenatal therapy [44]. Similar to findings in the foetal baboon lung, PTGER-2 was localized in the respiratory epithelium, mesenchyme and pulmonary vasculature[49]. The observed increase in PTGIR expression towards the end of gestation is congruent to findings in foetal human lungs[50].

The average transplacental passage of treprostinil into the foetal compartment was low (1.65%). Low foetal concentrations may be due to either a placental barrier effect, a back-transfer mechanism, placental or foetal hepatic metabolism, or a combination thereof. In human foetuses, treprostinil's primary metabolizing enzyme CYP2C8 is already expressed during the first trimester[51].

Clinically, treprostinil is titrated based on effect (pulmonary vasodilation), leaving no formal neonatal nor foetal concentration range to target. In our study in the nitrofen rat model of CDH, we therefore aimed to attain foetal concentrations above 0.5 ng/mL, which is the lowest reported effective (vasodilative) neonatal concentration[52]. However, we demonstrated that foetal concentrations of treprostinil below 0.5 ng/mL sufficed to exert treprostinil's anti-remodelling effect[2]. Similarly, in this rabbit study we observed that treprostinil concentrations lower than 0.025 ng/mL (C.T.50 and C.T.100), were already associated with biological activity, i.e. increased %MWT and increased glomerular maturation.

We performed a comprehensive analysis of maternal tolerance and foetal safety at different doses of treprostinil. Does exposed to treprostinil demonstrated temporary reduction of food consumption mainly on the day after drug initiation, an observation consistent with rabbit studies performed for the NDA of treprostinil[23]. We also observed pump site oedema of which the duration was congruent with the dose. In clinical studies investigating SC treprostinil administration, up to 85–92% of participants report incidental pump site reaction (swelling, redness, rash, and pain)[53,54]. Both the lesser food intake and the pump site oedema were temporary for all doses and were not associated with worse pain or neurobehavioral scores. Contrary to what studies in pregnant rabbits reported in treprostinil's NDA, we did not observe an increased incidence of a thirteenth rib in the offspring exposed to the same maternal dose of treprostinil (150 ng/kg/min). We speculate this is most likely due to the later administration of treprostinil in our study, well past the embryological developmental phase[23].

In foetuses exposed to treprostinil, we observed increased renal glomerular maturation. In human kidneys, PTGIR and PTGER-2 are abundantly expressed in the nephrogenic cortex[55,56]. The severely distorted renal glomerular, vascular, and interstitial development in PTGIS-knockout mice further confirms prostacyclin's vital role in normal renal development[55,57]. Antenatal corticosteroids have been demonstrated to similarly accelerate renal morphologic maturation in preterm baboons[58], which clinically resulted in improved renal function in neonatal life[59].

Prenatal treprostinil also affected pulmonary vascular development in control foetuses, increasing the arteriolar %MWT and thus creating a hypertensive phenotype. We also observed this phenomenon in rats with normal lung development prenatally exposed to treprostinil[2]. Similarly, prenatal exposure of control rats and rabbits to sildenafil, a phosphodiesterase 5 inhibitor with anti-remodelling effects, increased the %MWT and reduced vascular branching[60,61]. Although the mechanism behind these observations remains unclear, one could imagine that in response to the vasodilatory agent, the foetus mounts a

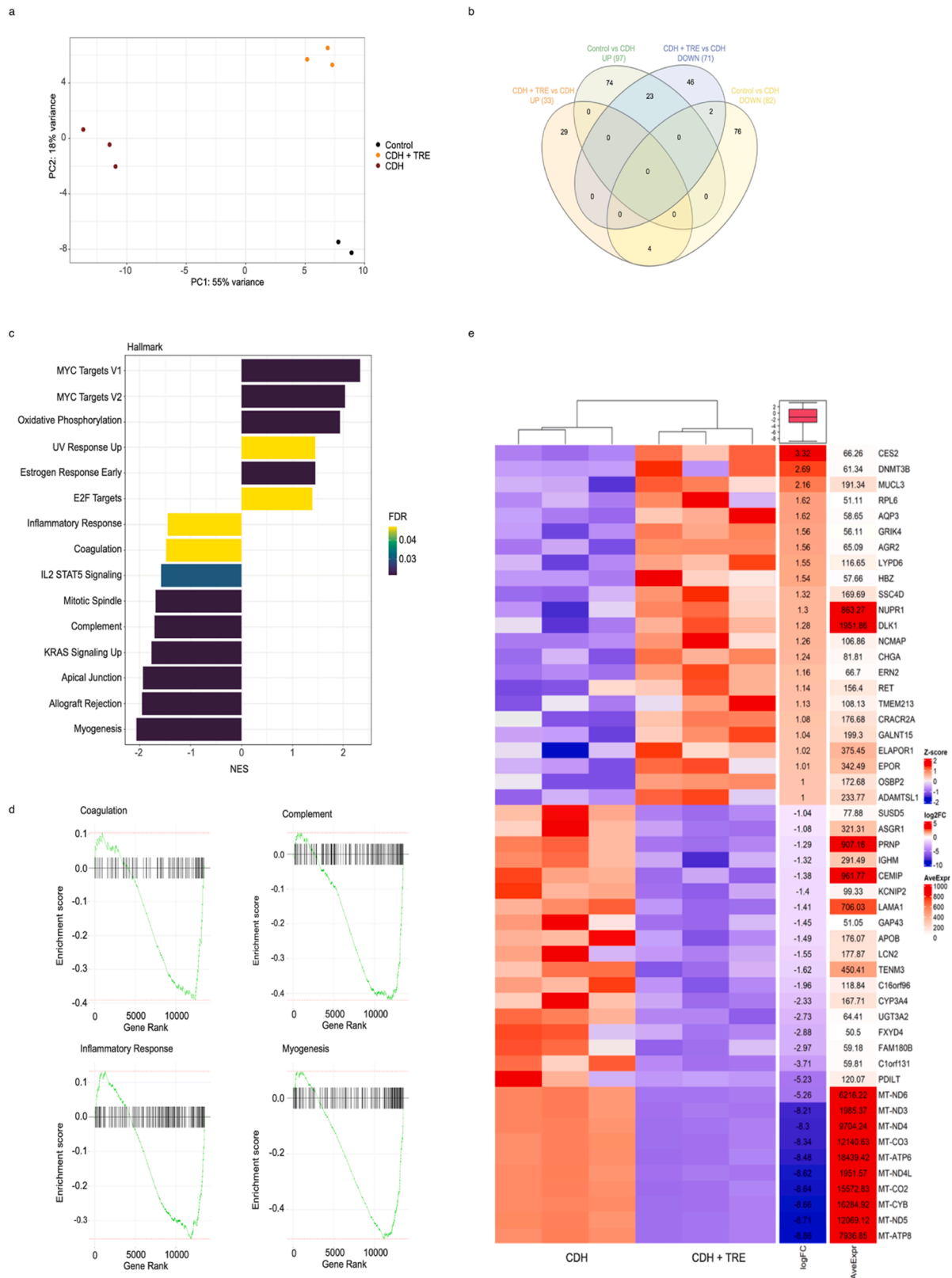


Fig. 8. Transcriptome analysis. a) Principle component analysis (PCA). b) Venn diagram displaying the number of deregulated genes. The genes are detailed in the supplemental table 3. c) Hallmark gene sets that are significantly enriched for genes that are up- or downregulated based on gene set enrichment analysis (GSEA; 5% FDR). d) Gene set enrichment plots of coagulation, complement, inflammatory response and myogenesis. e) Heatmap containing the 50 most up- and downregulated genes (selected by Log2FC) from CDH and CDH+TRE from three biological replicates per group. Colour represents row-scaled, normalized read counts. NES = normalized enrichment score.

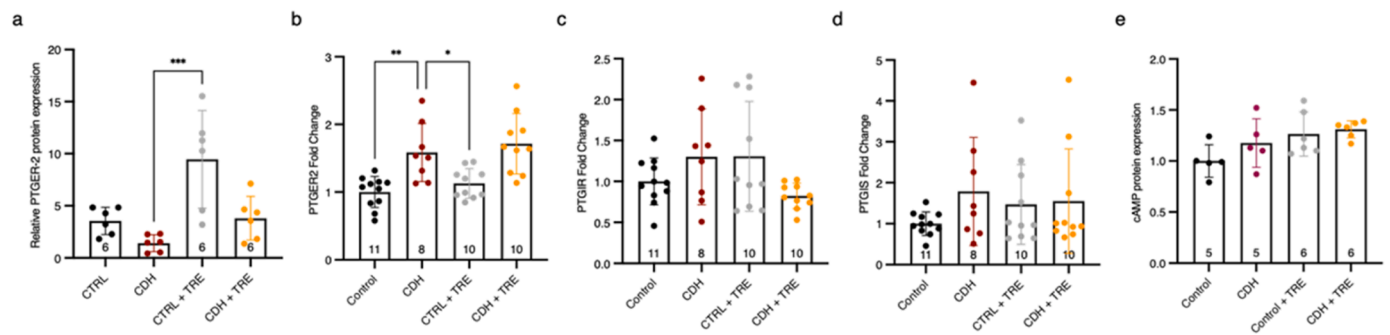


Fig. 9. Molecular pathway analysis. a PTGER-2 protein expression assessed by western blot and normalized for GAPDH expression. b PTGER-2 and c PTGIR mRNA fold change, qPCR. d RNA fold change of PTGIS (PTGIS-synthase), qPCR. e Protein expression of cyclic adenosine monophosphate (cAMP) by enzyme-linked immunosorbent assay (ELISA). Full lines represented means and error bars standard deviations. The number of biological replicates were indicated at the bottom of each bar. Data were compared using Dunnett's multiple comparison test with the CDH group as reference. * = $p < 0.05$, ** = $p < 0.01$, *** = $p < 0.001$.

compensatory vasoconstrictive reaction to restore minimal pulmonary circulation. Prolonged vasoconstriction may prevent the physiologic arteriolar thinning of the media towards the end of gestation, resulting in the relative hypermuscularization we and others have described [2,28,60,61]. Moreover, we have argued before that these structural vascular changes may provide at least a partial answer to the findings in the Dutch arm of STRIDER (*Sildenafil Therapy in Dismal Prognosis Early-Onset Foetal Growth Restriction*) trial [62,63]. This study investigating foetal sildenafil for severe foetal growth restriction was stopped early, after higher-than-expected neonatal mortality and persistent pulmonary hypertension of the new-born was noted upon interim analysis [64,65]. Wary of these findings, we infer that clinical trials with prenatal administration of treprostinil in conditions with normal lung development should be strongly dissuaded.

The rabbit model has been extensively used for the study of perinatal brain development resulting from prenatal insults, demonstrating histologic brain changes associated with neurobehavioral impairment after for example fetal surgery, antenatal corticosteroids, and fetal growth restriction [29,66,67]. We performed extensive histological brain analysis and did not find differences in treprostinil-exposed pups.

Treprostinil administration was started on GD24, during the early canalicular lung development phase. This timepoint is relevant since it correlates with a human equivalent of 18 weeks' gestation which is when CDH is usually diagnosed on prenatal ultrasound [44,68,69].

The primary outcome of this study was the %MWT of small pulmonary arterioles ($ID < 100 \mu m$, up to the pre-acinar vessels) which constitute the resistance vasculature of the lung [70]. The %MWT quantifies vascular muscularization and is a well-described hallmark of postnatal persistent PH [24,28,71–73]. Corroborating our findings in the nitrofen rat model, we found that the %MWT was lower in CDH+TRE pups than unexposed CDH pups, especially in the lower calibre pulmonary arterioles [2]. During normal lung development, progressive thinning of the media and adventitia is observed over the course of gestation in preparation for massive pulmonary vasodilation at birth [28]. Reversal of the hypermuscularized pulmonary arteriole phenotype observed in treprostinil-treated CDH pups would be predicted to attenuate the postnatal PH characteristic of this disorder.

Despite treprostinil's distinct effect on pulmonary arteriolar development, we did not observe an effect on alveolar morphometry, lung mechanics or overall ipsilateral lung hypoplasia. Although this confirms our findings in the rodent model of CDH, this contrasts with the findings of prenatal sildenafil in CDH [21,60]. While treprostinil and sildenafil act on different pathways (prostacyclin & nitric oxide pathways respectively), the timing of administration may also have played a role. Studies assessing prenatal experimental prostacyclin-analogues (NS-304 and ONO-1301SR) in the nitrofen-rat model have demonstrated improved airway development only when administered early, i.e. during the embryonic lung developmental phase (human equivalent of 4–7

weeks gestation) [44,74,75]. However, such early administration cannot be clinically translated since the clinical diagnosis of CDH is typically made on ultrasound, typically much later around gestational week 20 [69].

FETO is a clinically validated surgical procedure shown to stimulate prenatal pulmonary parenchymal development and to increase lung size in fetuses with CDH [5,6,24,76]. Treprostinil and FETO have complementary effects on prenatal lung development, and we speculate that when combined they could act synergistically, as was observed with sildenafil [9].

We also investigated the effect of treprostinil on pulmonary extracellular matrix (ECM) remodelling. cAMP, a down-stream regulator of treprostinil involved in ECM metabolism and proliferation control, trended slightly higher in treprostinil-exposed lungs. However, we did not observe decreased collagen type I deposition in pups exposed to treprostinil, which contrasts findings from in-vitro studies [16]. Concordantly, pulmonary functional characteristics (compliance, elastance, resistance and reactance) were not improved in pups with CDH after prenatal treprostinil exposure.

The positive enrichment of interferon alpha and gamma (both pro-inflammatory cytokines) we observed in lungs of pups with CDH is in line with a study demonstrating significantly increased levels of interferon alpha in cord blood of CDH neonates [77]. Others have suggested that inflammatory pathways play a crucial role in the pathophysiology of CDH and that anti-inflammatory agents may provide therapeutic benefit in CDH [78,79]. Treprostinil has an established anti-inflammatory effect that is reflected in the downregulation of gene sets involved in complement and inflammatory pathways (Fig. 9c). The downregulation observed in the myogenesis and coagulation pathway gene sets is consistent with treprostinil's other known mechanistic effects i.e. anti-remodelling and anti-aggregation respectively. Finally, the pattern of the observed pulmonary PTGER-2 protein expression perfectly reproduces the findings of our rat study [2].

This study has several limitations. First, the surgical rabbit CDH model only reproduces the thoracic compression caused by herniation of abdominal organs, not a potential primary insult prior to diaphragm development as hypothesized in the dual-hit hypothesis and reproduced in the nitrofen rat model [80]. Second, the timing of CDH creation and treatment nearly coincided, which is not ideal from a pathophysiological point of view. We did so to allow a sufficient long exposure given the short duration of rabbit gestation and to screen for a maximal effect of treprostinil, however accepting the risk to overestimate it. Third, we could not assess neonatal pulmonary pressures and blood gases, because in our experience rabbit pups cannot survive long enough due to the severe lung hypoplasia. Fourth, in an effort to reduce the number of animals needed, we harvested the contralateral, right lung for molecular analysis, and the ipsilateral, left lung for histology. Although both lungs are developmentally abnormal in CDH [81], the effect of local

compression is more pronounced in the ipsilateral lung [82]. The local effect on molecular and protein expression could therefore also be different from what we observed in the contralateral lung. Finally, we opted for continuous SC treprostinil administration for practical reasons, as it has the same bioavailability as IV administration [83]. Clinically, SC administration would be a burden to pregnant mothers. Alternatively, an extended-release oral formulation of treprostinil (Orenitram, United Therapeutics, Silver Springs, MD) was approved and is now available in the US [84].

Finally, although treprostinil does not improve airway in addition to pulmonary vascular development as seen with sildenafil, it has the critical advantage that it has not yet been investigated for any other prenatal indication. This allows the investigation to be targeted and to avoid a moratorium for clinical translation as is the case with sildenafil after the STRIDER-trial [2,85,86].

5. Conclusion

This study demonstrates that, in the rabbit, treprostinil's target receptors are present at relevant timepoints during gestation, and that prenatal treprostinil is well-tolerated by the does and fetuses. In rabbit pups with CDH, treprostinil effectively prevents hypermuscularization of pulmonary arterioles and downregulates pathways involved in myogenesis and inflammation. These findings are an important milestone towards clinical translation of treprostinil as an antenatal treatment to prevent pulmonary hypertension in CDH.

CRedit authorship contribution statement

Basurto David: Data curation. **Croubels Siska:** Formal analysis. **Regin Marius:** Formal analysis. **Partridge Emily:** Supervision, Writing – review & editing. **Cherlet Marc:** Formal analysis. **Regin Yannick:** Data curation, Formal analysis, Methodology. **Russo Francesca Maria:** Conceptualization, Data curation, Funding acquisition, Methodology, Resources, Supervision, Writing – review & editing. **De Bie Felix Rafael:** Conceptualization, Data curation, Formal analysis, Investigation, Methodology, Project administration, Visualization, Writing – original draft, Writing – review & editing. **Allegaert Karel:** Conceptualization, Methodology, Supervision, Writing – review & editing. **Scuglia Marianna:** Data curation, Formal analysis. **Dubois Antoine:** Data curation, Formal analysis, Methodology. **Deprest Jan:** Conceptualization, Funding acquisition, Investigation, Project administration, Supervision, Writing – review & editing. **Muylle Ewout:** Data curation, Formal analysis. **Arai Tomohiro:** Data curation, Formal analysis.

Declaration of Competing Interest

The authors declare that they have no known competing financial interests or personal relationships that could have appeared to influence the work reported in this paper.

Data availability

Data will be made available on request.

Acknowledgments

The authors would like to acknowledge Dr. Katrien De Clerq for assisting with placental morphometrical analysis, Dr. Tom Bleeser for assisting with the general anaesthesia procedures, Mrs. Katrien Luyten for histological processing, Ms. Sofie Jannes for conducting western blots, Ms. Rita Van Bree for conducting qPCR analysis and Mrs. Inge Bongaers for assisting with qPCR primer design. Treprostinil was quantified using an UHPLC-MS instrument part of the Ghent University MSmall Expertise Centre for advanced mass spectrometry analysis of small organic molecules. This work was supported by a grant to the KU

Leuven by CDH UK through Sparks (16KUL01). Felix R De Bie was funded by a Strategic Basic Research Grant from the Flanders Research Foundation (FWO – 1S31720N).

Data sharing statement

The authors All data will be made freely available upon written request addressed to the corresponding author. The raw data from our transcriptome analysis was deposited in the GEO repository (GSE220739) and will be accessible online upon publication: <https://www.ncbi.nlm.nih.gov/geo/query/acc.cgi?acc=GSE220739>.

Appendix A. Supporting information

Supplementary data associated with this article can be found in the online version at [doi:10.1016/j.biopha.2023.115996](https://doi.org/10.1016/j.biopha.2023.115996).

References

- [1] A. Zani, W.K. Chung, J. Deprest, M.T. Harting, T. Jancelewicz, S.M. Kunisaki, N. Patel, L. Antounians, P.S. Puligandla, R. Keijzer, Congenital diaphragmatic hernia, *Nat. Rev. Dis. Prim.* 8 (1) (2022), 37.
- [2] F.R. De Bie, C.G. Halline, T. Kotzur, K. Hayes, C.C. Rouse, J. Chang, A.C. Larson, S. A. Khan, A. Spina, S. Tilden, F.M. Russo, H.L. Hedrick, J. Deprest, E.A. Partridge, Prenatal treprostinil reduces the pulmonary hypertension phenotype in the rat model of congenital diaphragmatic hernia, *EBioMedicine* 81 (2022), 104106.
- [3] S. Kotecha, A. Barbato, A. Bush, F. Claus, M. Davenport, C. Delacourt, J. Deprest, E. Eber, B. Frenckner, A. Greenough, A.G. Nicholson, J.L. Anton-Pacheco, F. Midulla, Congenital diaphragmatic hernia, *Eur. Respir. J.* 39 (4) (2012) 820–829.
- [4] F.R. De Bie, C.M. Avitabile, L. Joyeux, H.L. Hedrick, F.M. Russo, D. Basurto, J. Deprest, N.E. Rintoul, Neonatal and fetal therapy of congenital diaphragmatic hernia-related pulmonary hypertension, *Arch. Dis. Child. -Fetal Neonatal Ed.* 107 (5) (2022) 458–466.
- [5] J.A. Deprest, K.H. Nicolaidis, A. Benachi, E. Gratacos, G. Ryan, N. Persico, H. Sago, A. Johnson, M. Wielgos, C. Berg, B. Van Calster, F.M. Russo, Randomized Trial of Fetal Surgery for Severe Left Diaphragmatic Hernia, *N. Engl. J. Med.* 385 (2) (2021) 107–118.
- [6] J.A. Deprest, A. Benachi, E. Gratacos, K.H. Nicolaidis, C. Berg, N. Persico, M. Belfort, G.J. Gardener, Y. Ville, A. Johnson, F. Morini, M. Wielgos, B. Van Calster, P.L.J. DeKoninck, Randomized trial of fetal surgery for moderate left diaphragmatic hernia, *N. Engl. J. Med.* 385 (2) (2021) 119–129.
- [7] A. Delabaere, L. Blanchon, K. Coste, G. Clairefond, C. Belville, P. Blanc, G. Marceau, V. Sapin, D. Gallot, Retinoic acid and tracheal occlusion for diaphragmatic hernia treatment in rabbit fetuses, *Prenat. Diagn.* 38 (7) (2018) 482–492.
- [8] M. Davey, S. Shegu, E. Danzer, E. Ruchelli, S. Adzick, A. Flake, H.L. Hedrick, Pulmonary arteriole muscularization in lambs with diaphragmatic hernia after combined tracheal occlusion/glucocorticoid therapy, *Am. J. Obstet. Gynecol.* 197 (4) (2007), 381 e1–7.
- [9] F.M. Russo, M. Cunha, J. Jimenez, F. Lesage, M.P. Eastwood, J. Toelen, J. Deprest, Complementary Effect of Maternal Sildenafil and Fetal Tracheal Occlusion Improves Lung Development in the Rabbit Model of Congenital Diaphragmatic Hernia, *Ann. Surg.* (2020).
- [10] F.M. Russo, P. De Coppi, K. Allegaert, J. Toelen, L. van der Veecken, G. Attilakos, M. P. Eastwood, A.L. David, J. Deprest, Current and future antenatal management of isolated congenital diaphragmatic hernia, *Semin Fetal Neonatal Med.* 22 (6) (2017) 383–390.
- [11] K.M. Lawrence, H.L. Hedrick, H.M. Monk, L. Herkert, L.N. Waqar, B.D. Hanna, W. H. Peranteau, N.E. Rintoul, R.K. Hopper, Treprostinil improves persistent pulmonary hypertension associated with congenital diaphragmatic hernia, *J. Pediatr.* 200 (2018) 44–49.
- [12] E. Carpentier, S. Mur, E. Aubry, L. Pognon, T. Rakza, F. Flamein, D. Sharma, P. Tourneux, L. Storme, Safety and tolerability of subcutaneous treprostinil in newborns with congenital diaphragmatic hernia and life-threatening pulmonary hypertension, *J. Pediatr. Surg.* 52 (9) (2017) 1480–1483.
- [13] U.T. Corporation, Remodulin Product Information, (2008).
- [14] F.R. De Bie, K. Allegaert, H.L. Hedrick, N.E. Rintoul, A. Davidson, Treprostinil attains clinically therapeutic concentrations in neonates with pulmonary hypertension on extracorporeal membrane oxygenation support, *Pharmacotherapy* (2020).
- [15] C. Lambers, M. Roth, P. Jaksch, G. Murakozy, M. Tamm, W. Klepetko, B. Ghanim, F. Zhao, Treprostinil inhibits proliferation and extracellular matrix deposition by fibroblasts through cAMP activation, *Sci. Rep.* 8 (1) (2018), 1087.
- [16] C. Lambers, C. Kornauth, F. Oberndorfer, P.M. Boehm, M. Tamm, W. Klepetko, M. Roth, Mechanism of anti-remodelling action of treprostinil in human pulmonary arterial smooth muscle cells, *PLoS One* 13 (11) (2018), e0205195.
- [17] J.A. Patel, L. Shen, S.M. Hall, C. Benyahia, X. Norel, R.J. McAnulty, S. Moledina, A. M. Silverstein, B.J. Whittle, L.H. Clapp, Prostanoid EP(2) Receptors Are Up-

- Regulated in Human Pulmonary Arterial Hypertension: a key anti-proliferative target for treprostinil in smooth muscle cells, *Int. J. Mol. Sci.* 19 (8) (2018).
- [18] N. Percie du Sert, V. Hurst, A. Ahluwalia, S. Alam, M.T. Avey, M. Baker, W. J. Browne, A. Clark, I.C. Cuthill, U. Dirnagl, M. Emerson, P. Garner, S.T. Holgate, D.W. Howells, N.A. Karp, S.E. Lazic, K. Lidster, C.J. MacCallum, M. Macleod, E. J. Pearl, O.H. Petersen, F. Rawle, P. Reynolds, K. Rooney, E.S. Sena, S. D. Silberberg, T. Steckler, H. Wurbel, The ARRIVE guidelines 2.0: updated guidelines for reporting animal research, *PLoS Biol.* 18 (7) (2020), e3000410.
- [19] J.S. Speed, K.A. Hyndman, In vivo organ specific drug delivery with implantable peristaltic pumps, *Sci. Rep.* 6 (1) (2016), 26251.
- [20] S.C. Keating, A.A. Thomas, P.A. Flecknell, M.C. Leach, Evaluation of EMLA cream for preventing pain during tattooing of rabbits: changes in physiological, behavioural and facial expression responses, *PLoS One* 7 (9) (2012), e44437.
- [21] F.M. Russo, J. Toelen, M.P. Eastwood, J. Jimenez, A.H. Miyague, G. Vande Velde, P. DeKoninck, U. Himmelreich, P. Vergani, K. Allegaert, J. Deprest, Transplacental sildenafil rescues lung abnormalities in the rabbit model of diaphragmatic hernia, *Thorax* 71 (6) (2016) 517–525.
- [22] M.C. Leach, S. Allweiler, C. Richardson, J.V. Roughan, R. Narbe, P.A. Flecknell, Behavioural effects of ovariectomy and oral administration of meloxicam in laboratory housed rabbits, *Res. Vet. Sci.* 87 (2) (2009) 336–347.
- [23] U.T. Company, *Pharmacology Review Part 1*, U.S. Food and Drug Administration, U.S. Department of Health & Human Services, 2002.
- [24] J. Wu, H. Yamamoto, E. Gratacos, X. Ge, E. Verbeke, K. Sueishi, S. Hashimoto, K. Vanamo, T. Lerut, J. Deprest, Lung development following diaphragmatic hernia in the fetal rabbit, *Hum. Reprod.* 15 (12) (2000) 2483–2488.
- [25] W. Scherle, A simple method for volumetry of organs in quantitative stereology, *Mikroskopie* 26 (1) (1970) 57–60.
- [26] T. Salaets, B. Tack, A. Gie, B. Pavie, N. Sindhwani, J. Jimenez, Y. Regin, K. Allegaert, J. Deprest, J. Toelen, A semi-automated method for unbiased alveolar morphometry: validation in a bronchopulmonary dysplasia model, *PLoS One* 15 (9) (2020), e0239562.
- [27] C.C.W. Hsia, D.M. Hyde, M. Ochs, E.R. Weibel, An official research policy statement of the American Thoracic Society/European Respiratory Society: standards for quantitative assessment of lung structure, *Am. J. Respir. Crit. Care Med.* 181 (4) (2010) 394–418.
- [28] X. Roubliova, E. Verbeke, J. Wu, H. Yamamoto, T. Lerut, D. Tibboel, J. Deprest, Pulmonary vascular morphology in a fetal rabbit model for congenital diaphragmatic hernia, *J. Pediatr. Surg.* 39 (7) (2004) 1066–1072.
- [29] J. van der Merwe, L. van der Veeken, A. Inversetti, A. Galgano, I. Valenzuela, T. Salaets, S. Ferraris, T. Vercauteren, J. Toelen, J. Deprest, Neurocognitive sequelae of antenatal corticosteroids in a late preterm rabbit model, *Am. J. Obstet. Gynecol.* 226 (6) (2022), 850.e1-850.e21.
- [30] T. Bleeser, L. Van Der Veeken, D. Basurto, I. Valenzuela, A. Brenders, L. Van Hoof, D. Emam, S. Vergote, M. Van de Velde, S. Devroe, J. Deprest, S. Rex, Neurodevelopmental effects of maternal blood pressure management with noradrenaline during general anaesthesia for nonobstetric surgery in the pregnant rabbit model, *Eur. J. Anaesthesiol.* 39 (6) (2022) 511–520.
- [31] P. Bankhead, M.B. Loughrey, J.A. Fernández, Y. Dombrowski, D.G. McArt, P. Dunne, S. McQuaid, R.T. Gray, L.J. Murray, H.G. Coleman, J.A. James, M. Salto-Tellez, P.W. Hamilton, QuPath: Open source software for digital pathology image analysis, *Sci. Rep.* 7 (1) (2017), 16878-16878.
- [32] J. Schindelin, I. Arganda-Carreras, E. Frise, V. Kaynig, M. Longair, T. Pietzsch, S. Preibisch, C. Rueden, S. Saalfeld, B. Schmid, J.-Y. Tinevez, D.J. White, V. Hartenstein, K. Eliceiri, P. Tomancak, A. Cardona, Fiji: an open-source platform for biological-image analysis, *Nat. Methods* 9 (7) (2012) 676–682.
- [33] A.E. Carpenter, T.R. Jones, M.R. Lamprecht, C. Clarke, I.H. Kang, O. Friman, D. A. Guertin, J.H. Chang, R.A. Lindquist, J. Moffat, P. Golland, D.M. Sabatini, CellProfiler: image analysis software for identifying and quantifying cell phenotypes, *Genome Biol.* 7 (10) (2006), R100-R100.
- [34] K. De Clercq, J. Lopez-Tello, J. Vriens, A.N. Sfruzzi-Perri, Double-label immunohistochemistry to assess labyrinth structure of the mouse placenta with stereology, *Placenta* 94 (2020) 44–47.
- [35] D. de Winter, T. Salaets, A. Gie, J. Deprest, E. Levchenko, J. Toelen, Glomerular developmental delay and proteinuria in the preterm neonatal rabbit, *PLoS One* 15 (11) (2020), e0241384.
- [36] T. Salaets, M. Aertgeerts, A. Gie, J. Vignero, D. de Winter, Y. Regin, J. Jimenez, G. Vande Velde, K. Allegaert, J. Deprest, J. Toelen, Preterm birth impairs postnatal lung development in the neonatal rabbit model, *Respir. Res.* 21 (1) (2020).
- [37] A.G. Gie, Y. Regin, T. Salaets, C. Casiraghi, F. Salomone, J. Deprest, J. Vanoirbeek, J. Toelen, Intratracheal budesonide/surfactant attenuates hyperoxia-induced lung injury in preterm rabbits, *Am. J. Physiol. Lung Cell Mol. Physiol.* 319 (6) (2020) L949–L956.
- [38] J.P. Decuyper, D. Van Giel, P. Janssens, K. Dong, S. Somlo, Y. Cai, D. Mekahli, R. Vennekens, Interdependent regulation of polycystin expression influences starvation-induced autophagy and cell death, *Int. J. Mol. Sci.* 22 (24) (2021).
- [39] T.D. Schmittgen, K.J. Livak, Analyzing real-time PCR data by the comparative CT method, *Nat. Protoc.* 3 (6) (2008) 1101–1108.
- [40] M.I. Love, W. Huber, S. Anders, Moderated estimation of fold change and dispersion for RNA-seq data with DESeq2, *Genome Biol.* 15 (12) (2014), 550.
- [41] X.I. Roubliova, J.A. Deprest, J.M. Biard, L. Ophalvens, D. Gallot, J.C. Jani, C.P. Van de Ven, D. Tibboel, E.K. Verbeke, Morphologic changes and methodological issues in the rabbit experimental model for diaphragmatic hernia, *Histol. Histopathol.* 25 (9) (2010) 1105–1116.
- [42] F. Faul, E. Erdfelder, A.G. Lang, A. Buchner, G*Power 3: a flexible statistical power analysis program for the social, behavioral, and biomedical sciences, *Behav. Res. Methods* 39 (2) (2007) 175–191.
- [43] B.J. Whittle, A.M. Silverstein, D.M. Mottola, L.H. Clapp, Binding and activity of the prostacyclin receptor (IP) agonists, treprostinil and iloprost, at human prostanoid receptors: treprostinil is a potent DP1 and EP2 agonist, *Biochem. Pharmacol.* 84 (1) (2012) 68–75.
- [44] J.C. Schittny, Development of the lung, *Cell Tissue Res.* 367 (3) (2017) 427–444.
- [45] A.W. Flemmer, J.C. Jani, F. Bergmann, O.J. Muensterer, D. Gallot, K. Hajek, J. Sugawara, H. Till, J.A. Deprest, Lung tissue mechanics predict lung hypoplasia in a rabbit model for congenital diaphragmatic hernia, *Pedia Pulmonol.* 42 (6) (2007) 505–512.
- [46] F.M. Russo, P. Mian, E.H. Krekels, K. Van Calsteren, D. Tibboel, J. Deprest, K. Allegaert, Pregnancy affects the pharmacokinetics of sildenafil and its metabolite in the rabbit, *Xenobiotica* 8 (1) (2018).
- [47] B. Fischer, P. Chavatte-Palmer, C. Viebahn, A. Navarrete Santos, V. Duranthon, Rabbit as a reproductive model for human health, *Reproduction* 144 (1) (2012) 1–10.
- [48] A.M. McArdle, K.M. Denton, D. Maduwegedera, K. Moritz, R.L. Flower, C. T. Roberts, Ontogeny of placental structural development and expression of the renin-angiotensin system and 11beta-HSD2 genes in the rabbit, *Placenta* 30 (7) (2009) 590–598.
- [49] T. Schmitz, L.A. Cox, C. Li, B.A. Levine, S.P. Ford, T.J. McDonald, P.W. Nathanielsz, Prostaglandin E2 receptor expression in fetal baboon lung at 0.7 gestation after betamethasone exposure, *Pedia Res* 61 (4) (2007) 421–426.
- [50] D.S. Mous, M.J. Buscop-van Kempen, R.M.H. Wijnen, D. Tibboel, R.J. Rottier, Changes in vasoactive pathways in congenital diaphragmatic hernia associated pulmonary hypertension explain unresponsiveness to pharmacotherapy, *Respir. Res.* 18 (1) (2017), 187.
- [51] M. Johansson, E. Strahm, A. Rane, L. Ekstrom, CYP2C8 and CYP2C9 mRNA expression profile in the human fetus, *Front. Genet* 5 (2014) 58.
- [52] K. Hall, M. Ogawa, C. Sakarovich, R.K. Hopper, G.T. Adamson, B. Hanna, D.D. Ivy, K. Miller-Reed, D. Yung, E. McCarthy, S.L. Siehr-Handler, J.A. Feinstein, Subcutaneous and Intravenous Treprostinil Pharmacokinetics in Children With Pulmonary Vascular Disease, *J. Cardiovasc. Pharmacol.* 73 (6) (2019) 383–393.
- [53] G. Simonneau, R.J. Barst, N. Galie, R. Naeije, S. Rich, R.C. Bourge, A. Keogh, R. Oudiz, A. Frost, S.D. Blackburn, J.W. Crow, L.J. Rubin, Continuous subcutaneous infusion of treprostinil, a prostacyclin analogue, in patients with pulmonary arterial hypertension, *Am. J. Respir. Crit. Care Med.* 165 (6) (2002) 800–804.
- [54] R.J. Barst, N. Galie, R. Naeije, G. Simonneau, R. Jeffs, C. Arneson, L.J. Rubin, Long-term outcome in pulmonary arterial hypertension patients treated with subcutaneous treprostinil, *Eur. Respir. J.* 28 (6) (2006) 1195–1203.
- [55] T. Klein, G. Klaus, M. Kömhoff, Prostacyclin synthesis: upregulation during renal development and in glomerular disease as well as its constitutive expression in cultured human mesangial cells, *Mediat. Inflamm.* 2015 (2015), 654151.
- [56] M.D. Breyer, L. Davis, H.R. Jacobson, R.M. Breyer, Differential localization of prostaglandin E receptor subtypes in human kidney, *Am. J. Physiol.* 270 (5 Pt 2) (1996) F912–F918.
- [57] R. Nasrallah, R.L. Hébert, Prostacyclin signaling in the kidney: implications for health and disease, *Am. J. Physiol. Ren. Physiol.* 289 (2) (2005) F235–F246.
- [58] L. Gubhaju, M.R. Sutherland, B.A. Yoder, A. Zulli, J.F. Bertram, M.J. Black, Is nephrogenesis affected by preterm birth? Studies in a non-human primate model, *Am. J. Physiol. Ren. Physiol.* 297 (6) (2009) F1668–F1677.
- [59] D. Cattarelli, G. Chirico, U. Simeoni, Renal effects of antenatally or postnatally administered steroids, *Pedia Med. Chir.* 24 (2) (2002) 157–162.
- [60] C. Luong, J. Rey-Perra, A. Vadevel, G. Gilmour, Y. Sauve, D. Koonen, D. Walker, K. G. Todd, P. Gressens, Z. Kassiri, K. Nadeem, B. Morgan, F. Eaton, J.R. Dyck, S. L. Archer, B. Thebaud, Antenatal sildenafil treatment attenuates pulmonary hypertension in experimental congenital diaphragmatic hernia, *Circulation* 123 (19) (2011) 2120–2131.
- [61] F.M. Russo, J. Toelen, M.P. Eastwood, J. Jimenez, A.H. Miyague, G. Vande Velde, P. DeKoninck, U. Himmelreich, P. Vergani, K. Allegaert, J. Deprest, Transplacental sildenafil rescues lung abnormalities in the rabbit model of diaphragmatic hernia, *Thorax* 71 (6) (2016) 517–525.
- [62] F.M. Russo, F.R. De Bie, E.A. Partridge, K. Allegaert, J. Deprest, The antenatal sildenafil STRIDER trial for severe fetal growth restriction, are post hoc reflections ad rem? *Eur. J. Pedia* (2022).
- [63] F.R. De Bie, D. Basurto, S. Kumar, J. Deprest, F.M. Russo, Sildenafil during the 2nd and 3rd Trimester of Pregnancy: trials and Tribulations, *Int J. Environ. Res Public Health* 19 (18) (2022).
- [64] K.M. Groom, W. Ganzevoort, Z. Alfrevic, K. Lim, A.T. Papageorghiou, Clinicians should stop prescribing sildenafil for fetal growth restriction (FGR): comment from the STRIDER Consortium, *Ultrasound Obstet. Gynecol.* 52 (3) (2018) 295–296.
- [65] A. Pels, J. Derks, A. Elvan-Taspinar, J. van Drongelen, M. de Boer, H. Duvekot, J. van Laar, J. van Eyck, S. Al-Nasiry, M. Sueters, M. Post, W. Onland, A. van Wassenaer-Leemhuis, C. Naaktgeboren, J.C. Jakobsen, C. Gluud, R.G. Duijnhoven, T. Lely, S. Gordijn, W. Ganzevoort, S.T.G. Dutch, Maternal sildenafil vs placebo in pregnant women with severe early-onset fetal growth restriction: a randomized clinical trial, *JAMA Netw. Open* 3 (6) (2020), e205323.
- [66] L. Van der Veeken, J. Van der Merwe, S. Devroe, A. Inversetti, A. Galgano, T. Bleeser, R. Meeusen, S. Rex, J. Deprest, Maternal surgery during pregnancy has a transient adverse effect on the developing fetal rabbit brain, *Am. J. Obstet. Gynecol.* 221 (4) (2019), 355.e1-355.e19.
- [67] I. Valenzuela, D. Basurto, Y. Regin, A. Gie, L. van der Veeken, S. Vergote, E. Muñoz-Moreno, B. Leszczynski, B. Tielemans, G.V. Velde, J. Deprest, J. van der Merwe, Placental vascular alterations are associated with early neurodevelopmental and pulmonary impairment in the rabbit fetal growth restriction model, *Sci. Rep.* 12 (1) (2022), 19720.

- [68] D. Gallot, C. Boda, S. Ughetto, I. Perthus, E. Robert-Gnansia, C. Francannet, H. Laurichesse-Delmas, J. Jani, K. Coste, J. Deprest, A. Labbe, V. Sapin, D. Lemery, Prenatal detection and outcome of congenital diaphragmatic hernia: a French registry-based study, *Ultrasound Obstet. Gynecol.* 29 (3) (2007) 276–283.
- [69] A. Syngelaki, T. Chelemen, T. Dagklis, L. Allan, K.H. Nicolaides, Challenges in the diagnosis of fetal non-chromosomal abnormalities at 11–13 weeks, *Prenat. Diagn.* 31 (1) (2011) 90–102.
- [70] J.M. Kay, Comparative morphologic features of the pulmonary vasculature in mammals, *Am. Rev. Respir. Dis.* 128 (2 Pt 2) (1983) S53–S57.
- [71] S.M. Shehata, D. Tibboel, H.S. Sharma, W.J. Mooi, Impaired structural remodelling of pulmonary arteries in newborns with congenital diaphragmatic hernia: a histological study of 29 cases, *J. Pathol.* 189 (1) (1999) 112–118.
- [72] R.L. Geggel, J.D. Murphy, D. Langleben, R.K. Crone, J.P. Vacanti, L.M. Reid, Congenital diaphragmatic hernia: arterial structural changes and persistent pulmonary hypertension after surgical repair, *J. Pediatr.* 107 (3) (1985) 457–464.
- [73] S.J. O'Toole, M.S. Irish, B.A. Holm, P.L. Glick, Pulmonary vascular abnormalities in congenital diaphragmatic hernia, *Clin. Perinatol.* 23 (4) (1996) 781–794.
- [74] D.S. Mous, H.M. Kool, P.E. Burgisser, M.J. Buscop-van Kempen, K. Nagata, A. Boerema-de Munck, J. van Rosmalen, O. Dzyubachyk, R.M.H. Wijnen, D. Tibboel, R.J. Rottier, Treatment of rat congenital diaphragmatic hernia with sildenafil and NS-304, selexipag's active compound, at the pseudoglandular stage improves lung vasculature, *Am. J. Physiol. -Lung Cell. Mol. Physiol.* 315 (2) (2018) L276–L285.
- [75] S. Umeda, S. Miyagawa, S. Fukushima, N. Oda, A. Saito, Y. Sakai, Y. Sawa, H. Okuyama, Enhanced pulmonary vascular and alveolar development via prenatal administration of a slow-release synthetic prostacyclin agonist in rat fetal lung hypoplasia, *PLoS One* 11 (8) (2016), e0161334.
- [76] J. Wu, X. Ge, E.K. Verbeken, E. Gratacós, N. Yesildaglar, J.A. Deprest, Pulmonary effects of in utero tracheal occlusion are dependent on gestational age in a rabbit model of diaphragmatic hernia, *J. Pediatr. Surg.* 37 (1) (2002) 11–17.
- [77] S. Fleck, G. Bautista, S.M. Keating, T.H. Lee, R.L. Keller, A.J. Moon-Grady, K. Gonzales, P.J. Norris, M.P. Busch, C.J. Kim, R. Romero, H. Lee, D. Miniati, T. C. MacKenzie, Fetal production of growth factors and inflammatory mediators predicts pulmonary hypertension in congenital diaphragmatic hernia, *Pedia Res.* 74 (3) (2013) 290–298.
- [78] R. Wagner, P. Lieckfeldt, H. Piyadasa, M. Markel, J. Riedel, C. Stefanovici, N. Peukert, D. Patel, G. Derrough, S.L. Min, J.-H. Gosemann, J. Deprest, C. D. Pascoe, A. Tse, M. Lacher, N. Mookherjee, R. Keijzer, Proteomic profiling of hypoplastic lungs suggests an underlying inflammatory response in the pathogenesis of abnormal lung development in congenital diaphragmatic Hernia, *Ann. Surg.* (2022), <https://doi.org/10.1097/SLA.0000000000005656>.
- [79] P.D. Losty, H.C. Suen, T.F. Manganaro, P.K. Donahoe, J.J. Schnitzer, Prenatal hormonal therapy improves pulmonary compliance in the nitrofen-induced CDH rat model, *J. Pediatr. Surg.* 30 (3) (1995) 420–426.
- [80] R. Keijzer, J. Liu, J. Deimling, D. Tibboel, M. Post, Dual-Hit hypothesis explains pulmonary hypoplasia in the nitrofen model of congenital diaphragmatic Hernia, *Am. J. Pathol.* 156 (4) (2000) 1299–1306.
- [81] F. Bargy, S. Beaudoin, P. Barbet, Fetal Lung Growth in Congenital Diaphragmatic Hernia, *Fetal Diagn. Ther.* 21 (1) (2005) 39–44.
- [82] F. Bargy, S. Beaudoin, P. Barbet, Fetal lung growth in congenital diaphragmatic hernia, *Fetal Diagn. Ther.* 21 (1) (2006) 39–44.
- [83] K. Laliberte, C. Arneson, R. Jeffs, T. Hunt, M. Wade, Pharmacokinetics and steady-state bioequivalence of treprostinil sodium (Remodulin) administered by the intravenous and subcutaneous route to normal volunteers, *J. Cardiovasc. Pharmacol.* 44 (2) (2004) 209–214.
- [84] P. Kumar, E. Thudium, K. Laliberte, D. Zaccardelli, A. Nelsen, A comprehensive review of treprostinil pharmacokinetics via four routes of administration, *Clin. Pharm.* 55 (12) (2016) 1495–1505.
- [85] F.R. De Bie, D. Basurto, S. Kumar, J. Deprest, F.M. Russo, Sildenafil during the 2nd and 3rd Trimester of Pregnancy: trials and tribulations, *Int. J. Environ. Res. Public Health* 19 (18) (2022) 11207.
- [86] K.M. Groom, W. Ganzevoort, Z. Alfirevic, K. Lim, A.T. Papageorghiou, S. Consortium, Clinicians should stop prescribing sildenafil for fetal growth restriction (FGR): comment from the STRIDER Consortium, *Ultrasound Obstet. Gynecol.* 52 (3) (2018) 295–296.